Available online at www.sciencedirect.com
ScienceDirect
Developmental Biology 297 (2006) 566–586
DEVELOPMENTAL BIOLOGY
www.elsevier.com/locate/ydbio

Genomes & Developmental Control

Tbx5-dependent rheostatic control of cardiac gene expression and morphogenesis

Alessandro D. Mori [a,b,c], Yonghong Zhu [a,c], Ilyas Vahora [a], Brian Nieman [d,e], Kazuko Koshiba-Takeuchi [a,c], Lorinda Davidson [d], Anne Pizard [f], J.G. Seidman [f], Christine E. Seidman [f,g], X. Josette Chen [d,e], R. Mark Henkelman [d,e], Benoit G. Bruneau [a,b,c,*]

[a] *Programmes in Cardiovascular Research and Developmental Biology, The Hospital for Sick Children, Toronto, ON, Canada M5G 1X8*
[b] *Department of Molecular and Medical Genetics, University of Toronto, Toronto, ON, Canada M5S 1A8*
[c] *The Heart and Stroke/Richard Lewar Centre of Excellence at the University of Toronto, Toronto, ON, Canada M5S 1A8*
[d] *The Mouse Imaging Centre (MICe), The Hospital for Sick Children, Toronto, ON, Canada M5G 1X8*
[e] *Department of Medical Biophysics, University of Toronto, Toronto, ON, Canada M5S 1A8*
[f] *Department of Genetics, Harvard Medical School and Howard Hughes Medical Institute, Boston, MA 02115, USA*
[g] *Division of Cardiology, Brigham and Women's Hospital, and Howard Hughes Medical Institute, Boston, MA 02115, USA*

Received for publication 16 January 2006; revised 8 May 2006; accepted 17 May 2006
Available online 24 May 2006

Abstract

Dominant mutations in the T-box transcription factor gene *TBX5* cause Holt–Oram syndrome (HOS), an inherited human disease characterized by upper limb malformations and congenital heart defects (CHDs) of variable severity. We hypothesize that minor alterations in the dosage of Tbx5 directly influences severity of CHDs. Using a mouse allelic series, we show a sensitive inverse correlation between *Tbx5* dosage and abnormal cardiac morphogenesis and gene expression. The CHDs found in mice harbouring a hypomorphic allele of *Tbx5* ($Tbx5^{lox/+}$ mice) are less pronounced than those found in *Tbx5* haploinsufficient mice ($Tbx5^{del/+}$), and homozygous hypomorphic ($Tbx5^{lox/lox}$) embryos have noticeably more advanced cardiac development than *Tbx5* null ($Tbx5^{del/del}$) embryos. Examination of target gene expression across the allelic series uncovers very fine sensitivity across the range of *Tbx5* dosages, in which some genes respond dramatically differently to only 15% differences in *Tbx5* mRNA levels. This analysis was expanded to a genome-wide level, which uncovered a *Tbx5* dosage-sensitive genetic program involving a network of cardiac transcription factors, developmentally important cell–cell signaling molecules, and ion channel proteins. These results indicate an exquisite sensitivity of the developing heart to *Tbx5* dosage and provide significant insight into the transcriptional and cellular mechanisms that are disrupted in CHDs.

Keywords: Tbx5; Rheostatic gradient; Holt–Oram syndrome; Transcription factor; Heart development; Optical projection tomography

Introduction

Cardiogenesis requires the coordinated development of many unique groups of cells that must precisely come together to form the elements that make up the adult heart. Such synchronicity is directed by precise patterns of gene expression that communicate information to cardiac precursors about the state of heart development, as well as their location with respect to other cells. Spatial and temporal information is ultimately communicated to the nucleus of developing heart cells by activation of specific sets of cardiac transcription factors (reviewed by Bruneau, 2002; Moorman et al., 2004; Mori and Bruneau, 2004; Srivastava and Olson, 2000).

Changes in the functional concentration of cardiac transcription factor proteins, due to dominant mutations in one allele (haploinsufficiency), can result in congenital heart defects (CHDs) in humans (Bruneau, 2002; Epstein and

* Corresponding author. Cardiovascular Research, The Hospital for Sick Children, 555 University Ave., Toronto, ON, Canada M5G 1X8. Fax: +1 416 813 7480.
E-mail address: bbruneau@sickkids.ca (B.G. Bruneau).

0012-1606/$ - see front matter © 2006 Elsevier Inc. All rights reserved.
doi:10.1016/j.ydbio.2006.05.023

Buck, 2000; Gruber and Epstein, 2004). The CHDs associated with DiGeorge Syndrome (OMIM #188400) and Holt–Oram syndrome (OMIM #142900) are caused by dominant mutations in the T-box transcription factor genes *TBX1* (Jerome and Papaioannou, 2001; Lindsay et al., 2001; Merscher et al., 2001; Yagi et al., 2003) and *TBX5* (Basson et al., 1997; Li et al., 1997; Mori and Bruneau, 2004), respectively. In addition, non-syndromic CHDs have been reported in families with dominant mutations in the homeobox transcription factor gene *NKX2-5* (Benson et al., 1999; Schott et al., 1998) and zinc-finger transcription factor gene *GATA4* (Garg et al., 2003; Okubo et al., 2004).

Work conducted to date examining the mechanistic basis behind Holt–Oram syndrome (HOS) has focused on describing the genetic and phenotypic changes resulting from Tbx5 haploinsufficiency (Basson et al., 1997; Bruneau et al., 2001; Li et al., 1997; Mori and Bruneau, 2004, and references therein). However, examination of phenotype is complicated by large variations in CHD severity of HOS clinical presentation, even between members of the same family. Attempts to correlate mutations in *TBX5* with severity of HOS manifestation have yielded mixed results but generally suggest that genetic modifiers influence CHD severity more than environmental or genotypic differences (Basson et al., 1999; Brassington et al., 2003; Huang et al., 2002).

Cis-regulatory modules frequently contain multiple sites for a single transcription factor (Davidson, 2002; Markstein et al., 2004) and required occupancy of multiple independent DNA-binding interactions would confer increased dosage sensitivity (Seidman and Seidman, 2002). Indeed, *Nppa* and *Gja5*, genes sensitive to Tbx5 dosage in mouse, have several Tbx binding sites in their regulatory regions (Bruneau et al., 2001, and unpublished data). We hypothesized that subtle alterations in Tbx5 dosage due to underlying genetic and/or environmental conditions may account for the variation in HOS manifestation and by extension that genes most sensitive to dosage would be altered in all HOS patients, whereas others would only show changes in a subset of severe cases. Understanding which genes are most sensitive to Tbx5 dosage and therefore most likely altered in the diseased state would be an important step in understanding and treating CHDs caused by transcription factor haploinsufficiency.

Tbx5 heterozygous null ($Tbx5^{del/+}$) mice recapitulate the CHDs seen in HOS patients whereas homozygous null mice ($Tbx5^{del/del}$) are growth arrested at E9.0 and die in utero by E10.5 due to severe heart defects (Bruneau et al., 2001). Here we show that the conditional allele ($Tbx5^{lox}$)–which was a precursor to the Cre-induced null allele–is hypomorphic, thus creating an allelic series based on dosage of *Tbx5*. Hypomorphic mutants exhibit milder defects than the respective null mutants, both in the heterozygous state as models of HOS, and as homozygous embryos with defective cardiac morphogenesis. Furthermore, we show that increases in CHD severity are linked to differential changes in expression of downstream targets of *Tbx5*. By gene expression profiling, we identify genes with variable sensitivity to *Tbx5* dosage and determine that Tbx5 is likely to regulate complex transcriptional networks. The exquisite sensitivity of downstream genes to *Tbx5* dosage provides a mechanistic explanation for the large differences in HOS clinical presentation; the identified targets provide an entry point to understanding the complex phenotypes caused by *Tbx5* haploinsufficiency.

Materials and methods

Animals

$Tbx5^{lox/+}$ and $Tbx5^{del/+}$ mice were generated and genotyped as previously described (Bruneau et al., 2001). For removal of the Neo^r gene, $Tbx5^{lox/+}$ mice were bred to EIIaCre mice (129SvJ strain; Jackson Laboratories, Bar Harbour, ME) and genotyped for the presence of *Tbx5* exon 3 and the absence of Neo^r using PCR. The EIIaCre was removed from the germ-line by breeding into 129SvEv and genotyping for the absence of Cre. This new mouse strain $Tbx5^{LDN/+}$ was bred 4 generations into 129SvEv before homozygous mice were generated. All methods performed on animals used in this study were approved by the Animal Care Committee of the Hospital for Sick Children.

In vivo electrocardiogram (ECG) telemetry collection

Twelve-week-old adult mice were anesthetized and EA-F20 telemetry device (Data Sciences International; St. Paul, MN) were implanted dorsally with electrodes in a lead II configuration. Mice were allowed to recover for 60 h post-surgery before ECG data were collected. Twenty measurements per ECG trace were collected during nocturnal activity (between 0:00 and 7:00) over at least two consecutive days. Data points were averaged to give a single value per mouse per parameter value examined. P wave width, P wave amplitude, PQ interval duration, QRS interval duration, QRS wave amplitude, ST interval duration, and heart rate were measured.

Magnetic resonance imaging (MRI) and optical projection tomography (OPT)

Mice were fixed for whole-body MRI by ultrasound guided left-ventricular catheterization as previously described (Zhou et al., 2004). MR images were subsequently obtained with a 40-cm bore, 7-T magnet (Magnex Scientific, Oxford, UK) operated by a UnityINOVA console (Varian NMR Instruments, Palo Alto, CA). We used a conventional three-dimensional spin-echo sequence with the following parameters: 300 ms repetition time, 10 ms echo time, (28 × 28 × 120) mm^3 field-of-view, and 420 × 420 × 1800 imaging matrix. Total imaging time was 14.7 h.

Optical projection tomography (OPT) was performed essentially, as described (Sharpe et al., 2002), on embryos fluorescently labeled by in situ hybridization against *Actc* and *Mybpc3* (Lickert et al., 2004). Visualization and manipulation of OPT data were performed with Amira 3.0 (Mercury Computer Systems Inc. Chelmsford, MA).

In situ hybridization

Whole-mount in situ hybridization was preformed according to standard protocols. Section in situ hybridization on paraffin sections was performed using modifications of the whole-mount in situ hybridization protocol.

Microarray analysis

Total RNA was isolated by TRIzol (Invitrogen, Carlsbad, CA) extraction from 14 to 20 pooled E11.5–E12.0 hearts and hybridized to Affymetrix MOE430A and MOE430B chips according to manufacturer's protocol. To reduce strain variations, the mice used for this experiment were kept in the same genetic background (50% 129SvEv, 50% Black Swiss). Three chip sets were run for RNA isolated from wild-type hearts, 3 for $Tbx5^{lox/+}$ and 4 for $Tbx5^{del/+}$. Statistical comparisons of chip data were performed using GC-Robust Multichip Analysis (ArrayAssist V2.6.1642.30743; Iobion Informatics, Toronto, CA.) (Irizarry et al., 2003; Wu

and Irizarry, 2004) with variance correction using two-tailed unpaired *t* tests against wild-type chips. A probe-set expression was considered altered if it had a $P < 0.05$ vs. wild type (unless stated otherwise). Hierarchical clustering was performed using SpotFire DecisionMaker software (Somerville, MA).

Quantitative real-time PCR

Total RNA was isolated from either whole embryos (E8.5) or isolated cardiac tissue (E12.5) using TRIzol reagent. Quantitative real-time PCR was performed using TaqMan probe sets (Applied Biosystems). Expression data were analyzed using the ΔΔCT method (Livak and Schmittgen, 2001). *GAPDH* was chosen as a control gene. The network represented in Fig. 9 was created using Biotapestry (Ver. 0.96.0) available at http://labs.systemsbiology.net/bolouri/software/BioTapestry/.

MULAN multispecies alignment

The mouse DNA sequence 25 kb upstream and 15 kb downstream (or until the start of the adjacent gene) of genes identified on microarray and confirmed altered in $Tbx5^{del/+}$ mutants using either quantitative real-time PCR or in situ hybridization were entered into the multisequence local alignment tool MULAN (http://mulan.dcode.org; Ovcharenko et al., 2005) along with the homologous sequences from the rat, dog, and human genomes (where available) to identify evolutionarily conserved domains likely to contain conserved transcription factor binding sites. Once the genomic regions were aligned, multi-TF transcription factor binding site analysis was performed using a predefined matrix similarity of 0.85 to the PWMs shown in Fig. 8A. Two adjacent Tbx5 sites or a Tbx5 site adjacent to an Nkx2.5 site separated by less than 500 bp was considered to be clustered. A *Tbx5*-insensitive gene is defined as a gene altered only in $Tbx5^{del/del}$ or $Tbx5^{lox/lox}$ mutants. A *Tbx5*-independent gene is defined as a gene known not to be altered in any *Tbx5* mutant.

Results

Identification of a Tbx5 hypomorphic allele

Previous work has shown that aberrant splicing into a neomycin resistance cassette (Neo^r) contained within the coding region of an active gene can result in the reduction or complete inactivation of gene expression (Meyers et al., 1998;

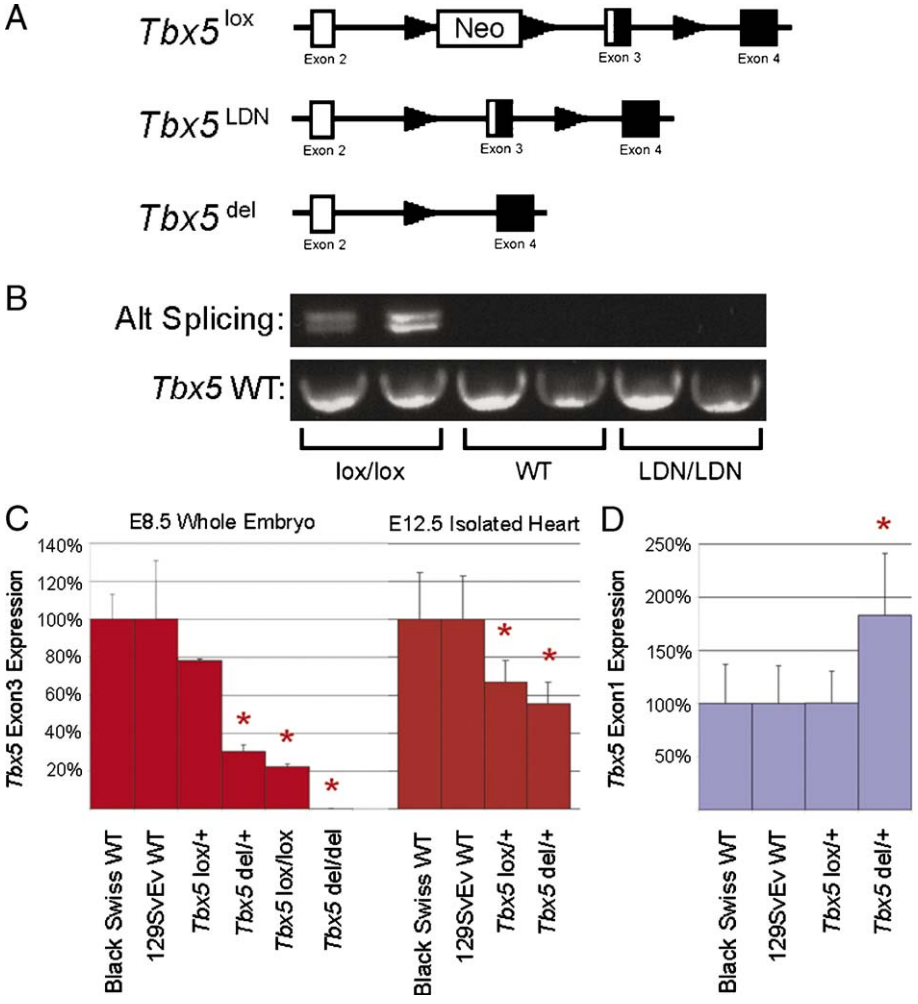

Fig. 1. The *Tbx5* allelic series (A) *Tbx5* alleles from the top to the bottom: $Tbx5^{lox}$, $Tbx5^{LDN}$, $Tbx5^{del}$; exons are indicated by roman numerals, open boxes show T-box encoding sequences and triangles are loxP sites. (B) Expression of aberrant transcripts from the $Tbx5^{lox}$ allele detected by RT-PCR at E10.5. Primers designed to amplify $Tbx5^{exon2}$–Neo^r hybrid mRNA detect two alternatively spliced transcripts from $Tbx5^{lox/lox}$ mRNA, which are absent from wild-type (WT) and $Tbx5^{LDN/LDN}$ mRNA (top bands). mRNA containing *Tbx5* exon 3 is amplified from mRNA from WT, $Tbx5^{lox/lox}$, and $Tbx5^{LDN/LDN}$ (bottom bands). (C) Quantitative real-time PCR analysis of *Tbx5*-exon 3 expression from either whole embryo lysate at E8.5 or isolated hearts at E12.5. Each mutant is normalized to its respective wild-type control. (D) Quantitative real-time PCR examining activity at the *Tbx5* locus by examining expression of *Tbx5*-exon 1 containing mRNA isolated from E12.5 hearts showing increased activity from the $Tbx5^{del}$ allele. $*P < 0.05$ versus WT.

Xu et al., 2001). The *Tbx5*^{lox} allele (Fig. 1A) contains a *Neo*^{r} used for embryonic stem cell selection (Bruneau et al., 2001). We hypothesized that *Tbx5*^{lox} might be a hypomorphic allele. Indeed, we could not recover live born *Tbx5*$^{lox/lox}$ mice from crosses of *Tbx5*$^{lox/+}$ animals (see below). To test whether aberrant splicing was occurring in transcripts made from the *Tbx5*^{lox} allele, primers were designed in exon 1 and the 3′ end of Neo^{r} (Supplemental Figure 1), and potential hybrid mRNAs containing both *Neo*^{r} and *Tbx5* sequences were amplified using reverse transcriptase-polymerase chain reaction (RT-PCR) (Fig. 1B). Two aberrantly spliced transcripts were seen in *Tbx5*$^{lox/lox}$ samples, in addition to normal *Tbx5* mRNA. Sequencing of these products confirmed erroneous splicing of normal *Tbx5* transcript after exon 2 into the *Neo*^{r} cassette. Both aberrant amplicons introduce stop codons into the primary *Tbx5* transcript shortly after splicing into *Neo*^{r} and would lack sequence encoding the T-box DNA binding motif of *Tbx5*; they are therefore presumed inactive. Alternative transcripts are absent in the wild-type control.

Selective removal of the *Neo*^{r} cassette created the new allele *Tbx5*^{LDN}, which retains functional loxP sites flanking *Tbx5* exon 3 (Fig. 1A). RT-PCR from *Tbx5*$^{LDN/LDN}$ RNA extracted at E10.5 shows only *Tbx5* mRNA with no alternatively spliced mRNA and thus is analogous to wild type (Fig. 1B). *Tbx5*$^{LDN/LDN}$ mice are viable and live for more than one year.

Allelic series created by conditional allele of Tbx5

Both *Tbx5*^{lox} and *Tbx5*^{del} alleles express mRNA containing *Tbx5* exons 1 and 2 but not exon 3. To quantitate levels of wild-type *Tbx5* mRNA production in mutant backgrounds, primers were designed across the exons 2–3 boundary to specifically amplify functional exon 3-containing *Tbx5* mRNA (Supplemental Figure 1). Quantitative real-time (qRT)-PCR was performed on RNA isolated from E8.5 embryos at the linear heart tube stage (before homozygous mutants die) and on RNA isolated from E12.5 hearts at the stage prior to cardiac septation in heterozygous mutants (Fig. 1C). The average amount of functional *Tbx5* transcripts in *Tbx5*$^{lox/+}$ mice is similar at E8.5 (78 ± 1% of WT) and E12.5 (67 ± 10% of WT) (P = N.S.). In contrast, *Tbx5*$^{del/+}$ embryos express 30 ± 3% wild-type *Tbx5* levels at E8.5 ($P < 0.005$ vs. WT), and expression increases to 55 ± 11% by E12.5 ($P < 0.06$ vs. E12.5 *Tbx5*$^{lox/+}$; $P < 0.005$ vs. WT). *Tbx5*$^{lox/lox}$ embryos at E8.5 have 22 ± 1% functional *Tbx5*, suggesting that splicing variants account for approximately 80% of all transcripts from the *Tbx5*^{lox} locus. No exon 3-containing *Tbx5* transcripts were detected from any of the *Tbx5*$^{del/del}$ embryos examined ($n = 8$). Reduced expression from the *Tbx5*^{lox} allele creates an allelic series based on decreasing dosage of *Tbx5* (from highest *Tbx5* expression to lowest: *Tbx5*$^{+/+}$ > *Tbx5*$^{lox/+}$ > *Tbx5*$^{del/+}$ > *Tbx5*$^{lox/lox}$ > *Tbx5*$^{lox/del}$ > *Tbx5*$^{del/del}$).

To confirm that the observed decreases in *Tbx5* expression were due to changes in the level of functional mRNA and not merely inactivity at the *Tbx5* locus, qRT-PCR was performed using primers designed to amplify Tbx5 exon 1-containing mRNA (expressed from both endogenous and mutant *Tbx5* alleles (see Supplemental Figure 1) to measure total activity from the *Tbx5* locus at E12.5 (Fig. 1D). Similar activity levels were observed between *Tbx5*$^{lox/+}$ embryos and the two wild-type strains. Unexpectedly, however, *Tbx5*$^{del/+}$ embryos showed a statistically significant increase in *Tbx5* exon 1-containing mRNA over its strain-matched wild-type control (183 ± 58% vs. 100 ± 37%; $P < 0.005$). As this increased activity was not accompanied by increased *Tbx5* exon 3 mRNA, we conclude that transcriptional activity was only increased from the null allele, which could suggest that the creation of the Cre-induced null allele removes a negative regulatory element and leads to a selective increase in this allelic variant of *Tbx5*.

Congenital heart defects in Tbx5 hypomorphic heterozygous mice

Crosses of *Tbx5*$^{lox/+}$ (129SvEv background) and wild-type 129SvEv mice yielded 42% *Tbx5*$^{lox/+}$ pups (76 of 180 examined; $P < 0.05$) at weaning suggesting that approximately 27% of *Tbx5*$^{lox/+}$ mice died prior to weaning. This phenotype is considerably milder than that seen in *Tbx5*$^{del/+}$ mice, which show greater than 90% perinatal death in a 129SvEv background (Bruneau et al., 2001), and 59% perinatal death in a Black Swiss outbred background (36 *Tbx5*$^{del/+}$ pups of 124 mice alive at weaning ($P < 0.001$ altered from the 50:50 expected ratio). In comparison, *Tbx5*$^{LDN/+}$ mice survived to weaning in Mendelian proportions (65 *Tbx5*$^{LDN/+}$ mice of 122 examined at weaning; P = N.S.) and lived for more than 1 year afterwards.

Cardiac defects in surviving *Tbx5*$^{lox/+}$ mice were assessed at 12 weeks of age by closed-chest magnetic resonance imaging (Figs. 2A–C). Atrial septal defects (ASDs) were found in all *Tbx5*$^{del/+}$ and *Tbx5*$^{lox/+}$ mice examined and all showed an enlargement of the atria consistent with the interatrial communications. Quantitation of ASD size indicated smaller ASDs in *Tbx5*$^{lox/+}$ mice compared to *Tbx5*$^{del/+}$ mice (Table 1). Wild-type and *Tbx5*$^{LDN/LDN}$ mice show no ASDs or cardiac dilation of any sort. No ventricular septal defects (VSDs) were observed in live heterozygous hypomorphic or null mutants.

Conduction system function of WT, *Tbx5*$^{lox/+}$, *Tbx5*$^{del/+}$, and *Tbx5*$^{LDN/+}$ mice at 12 weeks of age was examined using ECG telemetry over a 2-day period. A statistically significant increase in PQ-interval duration was measured in *Tbx5*$^{lox/+}$ hearts with respect to 129SvEv wild-type mice (37.1 ± 2.5 ms, $n = 5$ vs. 32.6 ± 0.7, $n = 4$, respectively; $P < 0.01$), indicative of first degree atrioventricular (AV) block (Table 1). This block is significantly less severe than that seen in *Tbx5*$^{del/+}$ mice (40.1 ± 1.3 ms, $P < 0.05$ vs. *Tbx5*$^{lox/+}$; $P < 0.0002$ vs. wild type). No other significant differences were observed for any other measurements. In addition, continuous monitoring of *Tbx5*$^{lox/+}$ mice over 48 h showed sporadic electrophysiological anomalies, including occurrences of ventricular tachycardia, sinus rhythm with premature atrial complexes, secondary degree AV block and sinoatrial (SA) pauses (Figs. 2D–G) similar to those previously reported in *Tbx5*$^{del/+}$ mice (Bruneau et al., 2001).

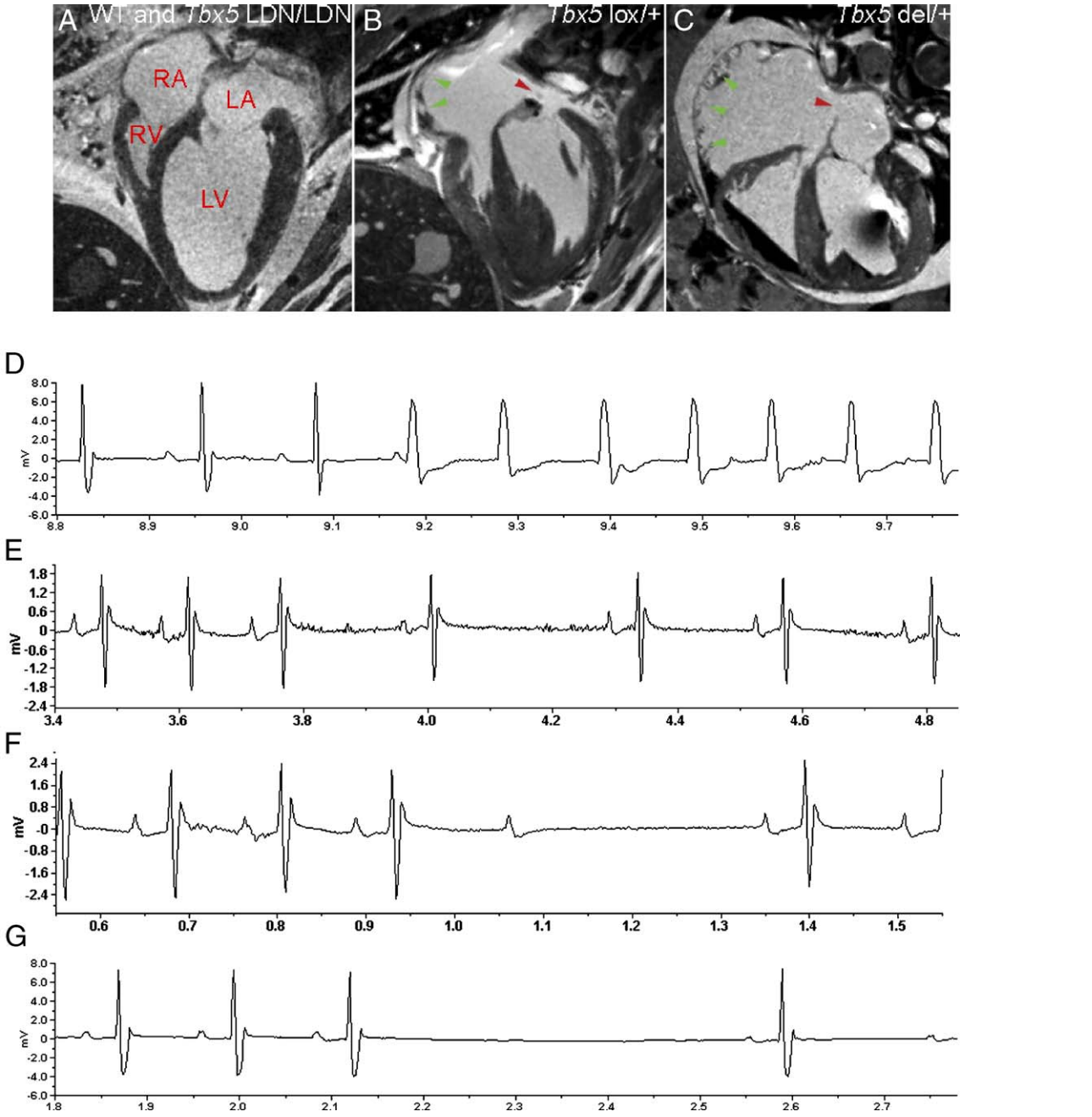

Fig. 2. Physical and physiological characterization of adult *Tbx5*$^{lox/+}$ and *Tbx5*$^{del/+}$ hearts (A–C) Closed-chested in vivo MRI images of 12-week-old mouse hearts. Representative MRI of a WT or *Tbx5*$^{LDN/LDN}$ heart (A) shows the normal septal divisions expected in the adult heart. Hearts of *Tbx5*$^{lox/+}$ (B) mice show small interatrial communications (red arrows) similar to those seen in *Tbx5*$^{del/+}$ mice (C). The changes in hemodynamics caused by these ASDs leads to dilatation of the atrial wall (green arrows). (D–G) Sporadic electrophysiological anomalies detected in *Tbx5*$^{lox/+}$ mice over continuous 24h recordings include occurrences of ventricular tachycardia (D), sinus rhythm with atrial complexes (E), second degree AV block (F), and sinoatrial (SA) pauses (G). Similar events were previously reported in *Tbx5*$^{del/+}$ mice (Bruneau et al., 2001).

Defects in heart formation in Tbx5 homozygous hypomorphic embryos

Tbx5$^{lox/lox}$ mice were growth arrested at E9.5 and died before E11.5 (Fig. 3A). *Tbx5*$^{lox/lox}$ hearts at E8.5 had a hypoplastic left ventricle (LV) and sinoatrial structures (primitive inflow track and atria) whereas the right ventricle (RV) and outflow track continued to develop, characteristic of *Tbx5*$^{del/del}$ heart development at the same stage (Figs. 3B–D). Optical projection tomography (OPT) imaging of E9.5 *Tbx5*$^{lox/lox}$ mutants illustrated that heart development was arrested at E9.0 (Figs. 3E–M). Although *Tbx5*$^{lox/lox}$ hearts had begun to loop, both atrial and ventricular structures were hypoplastic, lacking the left/right distinctions that are normally apparent at this stage. By comparison, E9.5 *Tbx5*$^{del/del}$ hearts had a single columnar ventricle projecting from the chest cavity, previously demonstrated to be outflow tract and RV (Bruneau et al., 2001), whereas posterior structures (atria and LV) were severely

Table 1
Summary of congenital heart defect severity across the *Tbx5* allelic series

	+/+	lox/+	del/+	lox/lox	del/del
Tbx5 dosage					
Functional *Tbx5* (exon 3)					
E8.5	100 ± 47% (129 SvEv) 100 ± 10% (BS)	78 ± 1%	30 ± 3%	22 ± 1%	0 ± 0%
E12.5	100 ± 10% (129 SvEv) 100 ± 19% (BS)	68 ± 10%	55 ± 11%	N/A	N/A
Survival					
	To birth, 100% survive at weaning	To birth, *129 SvEv*: 73% alive at weaning	To birth, *129 SvEv*: 10% alive at weaning *BS*: 40% alive at weaning	Death in utero by E11.5	Death in utero by E10.5
Cardiac structure					
12 weeks post-natal	Normal	ASD (100% of hearts)	ASD (100% of hearts)	N/A	N/A
ASD size (voxel dimensions standardized to spinal cord width)	N/A	93 ± 109	280 ± 5	N/A	N/A
E9.5	Normal	Indistinguishable from WT	Indistinguishable from WT	Hypoplastic atria, single ventricle	Severely hypoplastic ventricles and atria
E10.5	Normal	Indistinguishable from WT	Indistinguishable from WT	Bifurcated atrial tube, single ventricle	N/A
Electrophysiological					
PQ interval	32.59 ± 0.68 ms (129 SvEv) 2.45 ± 1.18 ms (BS)	37.09 ± 2.49 ms	40.10 ± 1.32 ms	N/A	N/A
Sporadic electrophysiological anomalies (3rd degree AV block, SA pauses, tachycardia, etc.)	Rare: 0–3 events per 24-h period	Common: up to 10 events per hour	Common: up to 10 events per hour	N/A	N/A

hypoplastic. By E10.5 (Figs. 3N–V), clear distinctions between the four chambers of the wild-type heart were evident, and the atrial septum and cardiac cushions were beginning to form. In contrast, $Tbx5^{lox/lox}$ hearts still had a tube-like atrium and single ventricle. A groove had now appeared that bisects the tube-like atrium (Fig. 3S). A separation between the two halves of this atrial tube was evident (Fig. 3V) coincident with the initial stages of separation of the common atrium into left and right atria. No live $Tbx5^{del/del}$ mutants have ever been recovered at E10.5, supporting our observations that $Tbx5^{lox/lox}$ embryos have less severe defects in heart formation than $Tbx5^{del/del}$ embryos.

Differential sensitivity of downstream genes to Tbx5 levels

Haploinsufficiency of *Tbx5* results in dramatic changes in gene expression. We have previously shown that expression of *Gja5* (encoding connexin 40) was reduced by 90% in hearts of $Tbx5^{del/+}$ mice, whereas expression of *Nppa* (encoding atrial natriuretic factor) was also decreased, albeit less dramatically (Bruneau et al., 2001). In *Tbx5* null embryos, decreased *Gata4*, *Myl2*, and *Irx4* was observed (Bruneau et al., 2001). Expression of these genes was assessed in our allelic series. It would be expected that mice with lower levels of *Tbx5* expression would display a proportional reduction in cardiac differentiation marker expression. However, changes in expression were not uniform across all genes examined. Rather, we observe that although the expression of some genes such as *Irx4* (Fig. 3A) and *Gata4* (Fig. 4B) was significantly reduced in $Tbx5^{lox/lox}$ embryos, expression of *Myl2* (Figs. 3B–D) was unchanged compared to wild-type littermates. Similarly, *Nppa* expression was not altered in E9.5 $Tbx5^{lox/+}$ embryos, whereas its expression was reduced in $Tbx5^{del/+}$ mice, as well as expanded across the interventricular septum. Such differences are manifest not only in changes throughout the entire heart but also in changes in expression within certain tissue types: *Gja5* expression was significantly reduced in the ventricles of $Tbx5^{lox/+}$ embryos at E9.5, whereas atrial expression of *Gja5* was maintained closer to wild-type levels (Fig. 4C).

Gene expression profiling identifies Tbx5 dosage-sensitive genes

The data presented above draw comparisons between distinct populations of mice subdivided on the basis of genotype to show a correlation between CHD severity and *Tbx5* dosage. However, subtle distinctions in phenotype are seen between individuals within a given subgroup due in part to variable *Tbx5* expression in genetically identical mice (Fig. 5A). Along this continuum of Tbx5 expression, it should be possible to differentiate genes that are highly sensitive to minor perturbations in *Tbx5* (whose expression would be affected in both mild ($Tbx5^{lox/+}$) and severe ($Tbx^{del/+}$) HOS cases) from those that are not as sensitive (and are therefore only affected in a subset of severe HOS cases). To this

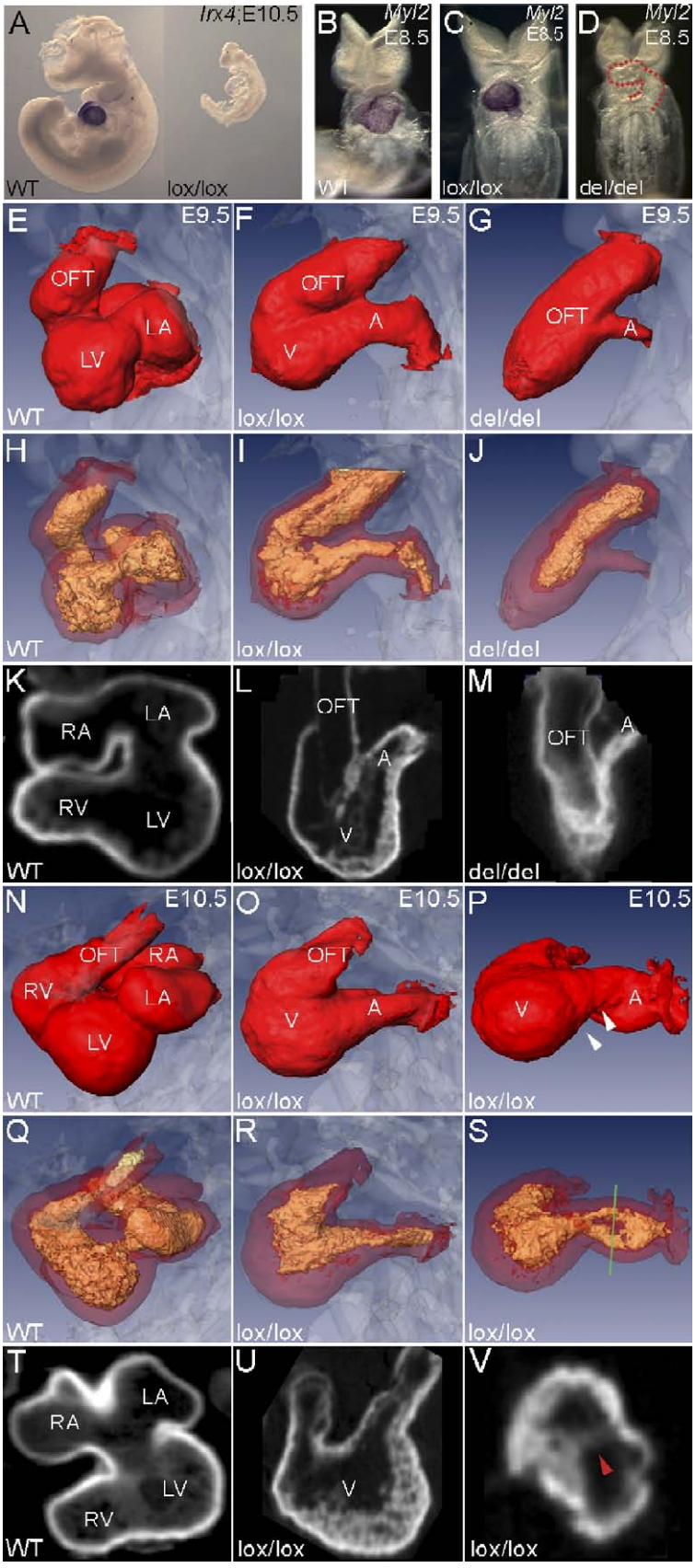
A
Irx4;E10.5
WT
lox/lox
B
Myl2
E8.5
WT
C
Myl2
E8.5
lox/lox
D
Myl2
E8.5
del/del
E
E9.5
OFT
LA
LV
WT
F
E9.5
OFT
A
V
lox/lox
G
E9.5
OFT
A
del/del
H
WT
I
lox/lox
J
del/del
K
LA
RA
RV
LV
WT
L
OFT
A
V
lox/lox
M
OFT
A
del/del
N
E10.5
OFT
RA
RV
LA
LV
WT
O
E10.5
OFT
V
A
lox/lox
P
E10.5
V
A
lox/lox
Q
WT
R
lox/lox
S
lox/lox
T
LA
RA
LV
RV
WT
U
V
lox/lox
V
lox/lox

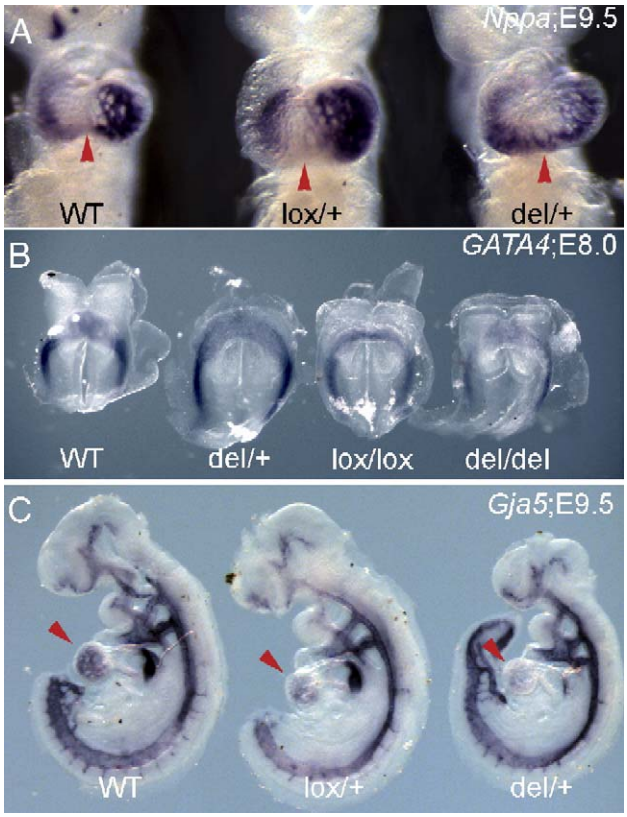

Fig. 4. Whole-mount in situ hybridizations showing gene expression changes for known genes downstream of *Tbx5*. (A) a ventral view showing unchanged *Nppa* expression in $Tbx5^{lox/+}$ embryos at E9.5. Prominent *Nppa* expression is seen in the LV of both wild-type and $Tbx5^{lox/+}$ embryos and is absent from the interventricular septum (red arrows). In contrast, *Nppa* expression is reduced in the $Tbx5^{del/+}$ embryos and is expanded across the interventricular septum. (B) Ventral view of *Gata4* expression at E8.5 showing decreased expression throughout the cardiac crescent of $Tbx5^{lox/lox}$ and $Tbx5^{del/del}$ embryos. (C) Lateral view of E9.5 embryos showing decreased expression of *Gja5* specifically in the LV of $Tbx5^{lox/+}$ mutants to a similar extent as in the heterozygous null embryo. Atrial expression levels of *Gja5* appear unchanged.

end, microarray analysis was performed using RNA isolated from pooled E11.5–12.0 embryos (WT, $Tbx5^{lox/+}$, and $Tbx5^{del/+}$) in order to assess the sensitivity of different genetic pathways to varying dosages of *Tbx5*. To minimize strain-specific variation, all embryos were of a mixed background (50% 129SvEv/50% Black Swiss), and pools of 14–20 hearts further minimized individual variation due to strain or minor staging differences. Affymetrix MOE430A and MOE430B chips were used to analyze the expression over 45,265 Unigene clusters ($n = 3$ WT pools, 3 $Tbx5^{lox/+}$ pools, and 4 $Tbx5^{del/+}$ pools). After applying GC-Robust Multichip Analysis (GC-RMA), we identified 177 genes as having significantly altered gene expression: 94 of these genes are significantly altered in both $Tbx5^{lox/+}$ and $Tbx5^{del/+}$ mice (these genes represent highly sensitive *Tbx5* gene targets, likely to be affected in all HOS patients), whereas the other 83 showed changes only in $Tbx5^{del/+}$ mice (these genes represent moderately sensitive gene targets, likely altered in only a subset of HOS patients). Of the initial 177 genes, only 98 showed strong changes in expression (greater than $\log_2 = \pm 0.3$: defined as the minimum threshold of expression needed for independent validation by quantitative real-time PCR in our hands) (shown in Fig. 5B). Among these 98 genes is *Gja5*, a direct target of Tbx5 that is known to be affected by *Tbx5* haploinsufficiency (Bruneau et al., 2001). Furthermore, because changes in expression of downstream targets are expected to be small, we also looked at those hits with slightly higher *P* values ($0.05 < P < 0.10$) to look for obvious cardiac genes potentially falsely eliminated by the stringent GC-RMA screen. We noted that the cardiac transcription factor genes *Hand1*, *Irx2*, and *Shox2*, the putative Wnt antagonist gene *Dkk3*, and the signaling molecule *Slit2* were measured as having downregulated expression (expression changes >log2 = ±0.3) in both $Tbx5^{lox/+}$ and $Tbx5^{del/+}$ mice just short of the $P < 0.05$ cutoff ($P = 0.0513$, 0.0565, 0.0603, 0.0785, 0.0961, respectively, vs. WT). Given that all five genes are expressed in the heart, and may be involved in pathways related to Tbx5 function, we included them as putatively downregulated pending further experimentation, bringing the number of gene altered in $Tbx5^{del/+}$ hearts to 182 and the number of highly sensitive genes to 99.

Classification of the 182 microarray genes into gene ontology (GO) categories revealed predominant downregulations of expression of transcriptional regulators (22%) and signal transduction molecules (14%), whereas metabolic genes were predominantly increased (18%) (Fig. 5C). By comparison, classification by GO annotation across the entire 45,290 probe set database showed that transcriptional regulation and signal transduction are only represented at a rate of 5.8% and 4.4%, respectively. Whereas highly sensitive Tbx5-regulated genes account for only 99 of 182 genes altered in $Tbx5^{del/+}$ mice, the relative ratios between functional classes of genes affected were maintained, suggesting that no single functional class of gene is more sensitive to changes in Tbx5 dosage (Tables 2 and 3).

To independently confirm changes in expression of genes identified above, we used whole-mount in situ hybridization at E10.5 and section in situ hybridization at E11.5 to screen for

Fig. 3. Heart development in homozygous mutants. (A) $Tbx5^{lox/lox}$ embryos at E10.5 are growth retarded compared to wild-type littermates. *Irx4* expression (blue) is decreased in $Tbx5^{lox/lox}$ embryos at this stage. (B–D) $Tbx5^{lox/lox}$ embryos at E8.5 (C) have hypoplastic left ventricle (LV) and sinoatrial structures (primitive inflow track and atria) whereas the right ventricle (RV) and outflow track continue to develop, characteristic of $Tbx5^{del/del}$ heart development (D). *Myl2* expression is maintained in $Tbx5^{lox/lox}$ embryos (blue) whereas it is undetectable in $Tbx5^{del/del}$ embryos. (E–M) Surface-rendered views of OPT on E9.5 WT, $Tbx5^{del/del}$, and $Tbx5^{lox/lox}$ embryos; heart is red, embryo is translucent white. E9.5 $Tbx5^{del/del}$ embryo outflow tract growth continues whereas LV and atrial structures are almost non-existent (Bruneau et al., 2001). By comparison, $Tbx5^{lox/lox}$ hearts have more developed posterior cardiac structures (H–J). Inner lumen of the hearts (yellow) are rendered in panels E–G. (K–M) Virtual sections through hearts shown in panels E–G. (N–V) OPT images of E10.5 $Tbx5^{lox/lox}$ hearts compared to wild type. $Tbx5^{lox/lox}$ hearts still have a tube-like atrium and single ventricle. A groove has appeared that bisects the tube-like atrium (white arrows in panel P). (Q–S) Inner lumen of hearts (yellow) are rendered in panels N–P. Examination of the cavity below the groove seen in Fig. 3P shows a physical separation between the two halves of this atrial tube. (T–V) Virtual sections through hearts shown in panels N–P. Virtual section through the heart in panel S (plane parallel to the green line) shows the development of a connection between the two halves of the single atria.

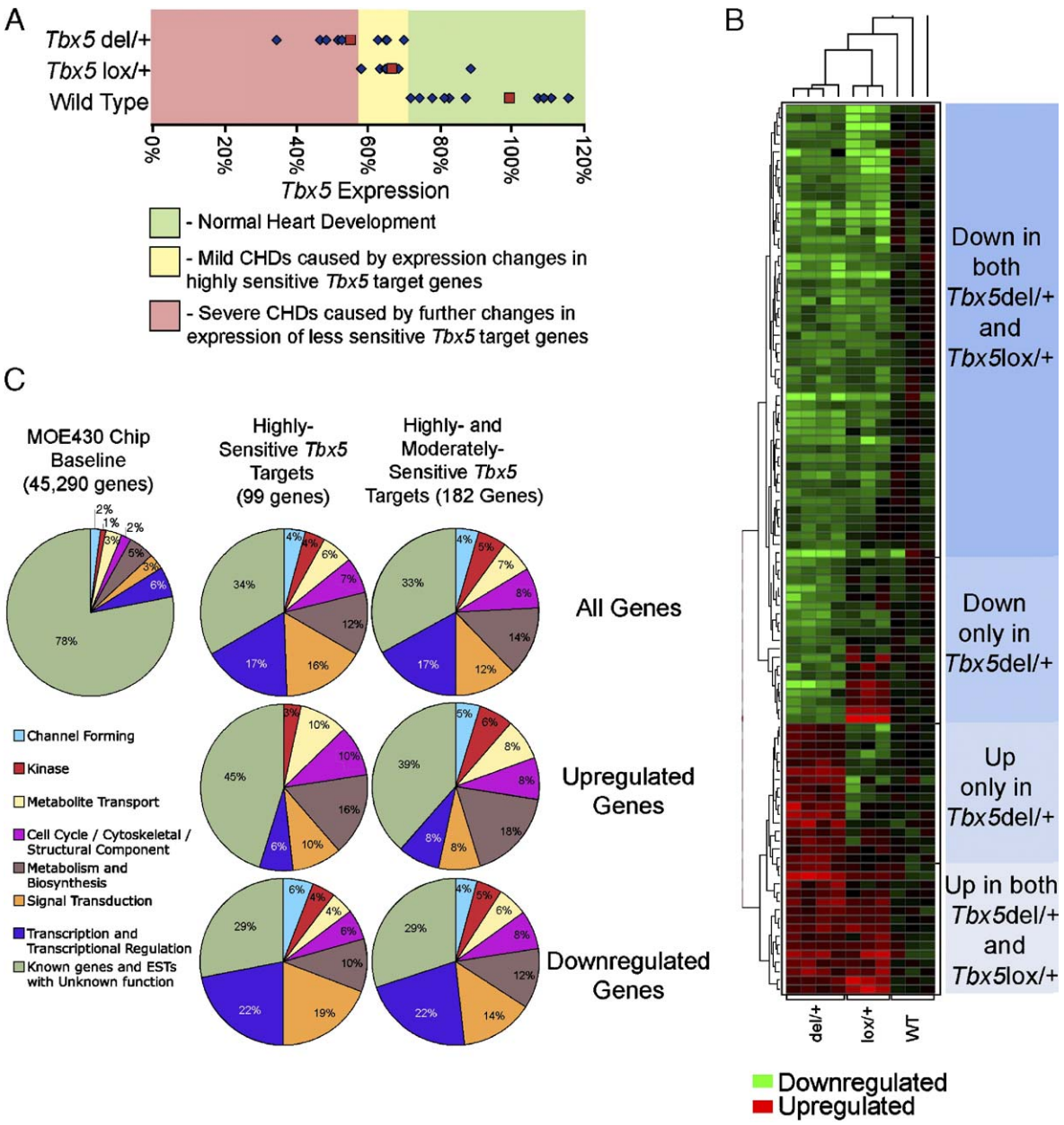

Fig. 5. (A) When individual *Tbx5* expression levels from the E12.5 embryos used to generate Fig. 1C (diamond) are visualized, they make up a continuum of *Tbx5* expression. Within this continuum, we see both mild CHDs (predominant in $Tbx5^{lox/+}$ mice) and more severe CHDs (predominant in $Tbx5^{del/+}$ mice). The average expression is represented by the red box. (B) Cluster analysis of the 102 genes identified as being differentially expressed by microarray with expression changes greater than $\log_2 = \pm 0.3$. Genes are clustered using a hierarchical clustering algorithm based in absolute expression changes verses wild type. (C) Pie charts examining the distribution of functional classes (based on classification by gene ontology (GO) annotations) among the 99 highly *Tbx5*-dosage-sensitive genes, as well as among the complete 182 gene set show predominant downregulations in transcriptional regulators (22%) and signal transduction (14%), whereas metabolic genes are predominantly increased. Distribution of the 45K gene clusters on the MOE430 gene chips is also shown.

changes in expression of 12 putative downstream targets (*2610024A01Rik*, *Agpat3*, *Ddx52*, *Dkk3*, *Eya1*, *Fbx032*, *Hand1*, *Hk1*, *Slit2*, *Tbx3*, *Vsnl1*, *Wisp1*) in $Tbx5^{del/+}$ mutants. All 12 genes were expressed in the heart, and 8 of these (*2610024A01*, *Ddx52*, *Dkk3*, *Eya1*, *Fbx032*, *Hk1*, *Vsnl1*, *Wisp1*) were also expressed in the limbs. Obvious changes were seen in the expression of 7 genes (*Dkk3*, *Fbxo32*, *Hand1*, *Hk1*, *Slit2*, *Tbx3*, *Wisp1*), consistent with that seen on the microarray (Fig. 6). In addition, expansion of *Wisp1* expression was noted across the interventricular septum (Fig. 6F). Changes in the expression of *Agpat3* (Fig. 6A) and *Ddx52* (data not shown) were noted opposite to that reported by microarray. The remainder of genes showed no appreciable change in expression by in situ.

Gene expression kinetics

A more sensitive screen of the microarray data was performed with qRT-PCR by examining the expression of 17 genes using RNA from individual E12.5 hearts; 12 genes

Table 2
Highly sensitive *Tbx5* dose-dependant genes (altered in both $Tbx5^{lox/+}$ and $Tbx5^{del/+}$)

Up/down[A]	Gene symbol	Gene title	Proposed biological functions	Unigene code
Cell cycle				
d	Mcm2	Minichromosome maintenance-deficient 2 mitotin (*S. cerevisiae*)	Involved in DNA replication and cell division	Mm.16711
Cellular/structural component				
d[a]	Lamp1	Lysosomal membrane glycoprotein 1	Lysosomal membrane glycoprotein; unknown biological function	Mm.16716
D	Mtdh	Metadherin	Nuclear membrane-associated protein; unknown biological function	Mm.130883
U[a]	Mrps25	Mitochondrial ribosomal protein S25	Structural component of ribosome	Mm.87062
U	Pscd1	Pleckstrin homology, Sec7 and coiled-coil domains 1	Membrane protein; unknown biological function	Mm.86413
Channel-forming proteins				
D[a]	Cacna2d2	Calcium channel, voltage-dependent, alpha 2/delta subunit 2	Sympathetic regulation of cardiac conduction	Mm.100236
D[b]	Cx40	Gap junction membrane channel protein alpha 5	Gap junction protein involved in cardiac conduction	Mm.281816
D[b]	Kcna5	Potassium voltage-gated channel, shaker-related subfamily, member 5	Potassium channel involved in I(K,Slow1) current during cardiac conduction	Mm.222831
d[a]	Ttyh3	Tweety homolog 3	Large conductance chloride channel; potential role in Ca signaling	Mm.28947
Cytoskeletal				
D	Dal1	Erythrocyte protein band 4.1-like 3	Actin binding protein; unknown biological function	Mm.132761
u	Mapt	Microtubule-associated protein tau	Microtubule-associated protein enriched in axons; unknown biological function	Mm.1287
Kinase				
D	Acp6	Acid phosphatase 6, lysophosphatidic	Acid phosphatase; unknown biological function	Mm.101368
D	Clk4	CDC like kinase 4	Kinase; potential involvement in the ubiquitination pathway	Mm.239354
D	Etnk1	Ethanolamine kinase 1	Ethanolamine kinase; unknown biological function	Mm.272548
U[c]	Yes	Yamaguchi sarcoma viral (v-yes) oncogene homolog	Src kinase family member; unknown biological function	Mm.4558
Metabolism and biosynthesis				
D[b]	Cdo1	Cysteine dioxygenase 1, cytosolic	Dioxygenase involved in taurine biosynthesis	Mm.241056
D	Cryl1	Crystalline, lambda 1	Oxoreductase; unknown biological function	Mm.25539
d	Iars2	Isoleucine-tRNA synthetase 2, mitochondrial	tRNA aminoacylation	
D	Lyzs	Lysozyme	Catabolic enzyme; unknown biological function	Mm.45436
D	Nudt11	Nudix (nucleoside diphosphate linked moiety X)-type motif 11	Phosphohydrolase; unknown biological significance	Mm.41198
D[a]	Ogt	*O*-linked *N*-acetylglucosamine (GlcNAc) transferase	Transcriptional repressor complex component; immune function	Mm.259191
D	Prss35	Protease, serine, 35	Protease; unknown biological function	Mm.257629
D	Wfdc1	WAP four-disulfide core domain 1	Endopeptidase; unknown biological activity	Mm.87599
u	Bak1	BCL2 antagonist/killer 1	Activator of caspases and involved in apoptosis	Mm.2443
u[a]	Cox15	COX15 homolog, cytochrome *c* oxidase assembly protein	Oxidative metabolism; ATP synthesis	Mm.248237
U[b]	Ddc	Dopa decarboxylase	Catecholamine metabolism	Mm.12906
U	Hibch	3-Hydroxyisobutyryl-coenzyme A hydrolase	Hydrolase; unknown biological function	Mm.222063
u[a]	Trnt1	tRNA nucleotidyl transferase, CCA-adding, 1	tRNA nucleotidyltransferase; unknown biological function	Mm.196332
Metabolite transport				
D	Copg2	Coatomer protein complex, subunit gamma 2	Protein transporter complex; unknown biological function	Mm.335639
D	Stx17	Syntaxin 17	Unknown biological function	Mm.171334
D	Stx8	Syntaxin 8	Vesicular trafficking and docking	Mm.39095
U	Cubn	Cubilin (intrinsic factor-cobalamin receptor)	Receptor involved in endocytosis	Mm.313915

(continued on next page)

Table 2 (*continued*)

Up/down[A]	Gene symbol	Gene title	Proposed biological functions	Unigene code
Metabolite transport				
u[a]	Hsdl2	Hydroxysteroid dehydrogenase like 2 (Hsdl2)	Sterol carrier activity; unknown biological activity	Mm.272905
U	Usp13	Ubiquitin-specific protease 13	Small ubiquitin-related modifier-mediated nuclear import	Mm.316153
Signal transduction				
D[b]	Cxxc4	CXXC finger 4; Idax	Negative regulator of Wnt signaling	Mm.224814
D[b, d]	Dkk3	Dickkopf homolog 3 (*Xenopus laevis*)	Secreted inhibitor of Wnt signaling	Mm.55143
D[b]	Fbxo32	F-box only protein 32	Ubiquitin ligase; inhibitor of calcineurin-induced hypertrophy	Mm.292042
D	Gnb4	Guanine nucleotide binding protein, beta 4	G-protein coupled receptor; unknown biological function	Mm.139192
d	Gsk3b	Glycogen synthase kinase 3 beta	Signaling molecule in the Wnt/beta-catenin pathway	Mm.200770
d	Hhat	Hedgehog acetyltransferase	Palmitoylation of *Drosophila* Hh needed for secretion; Hedgehog signaling pathway	Mm.145857
d	Igfbp5	Insulin-like growth factor binding protein 5	Insulin-like growth factor regulation of cell growth; binds specifically with Fhl2, also downregulated	Mm.309617
d[a]	Lnk	Linker of T-cell receptor pathways	Adaptor protein modulating hematopoietic progenitor cell differentiation	Mm.65493
d	Lnx1	Ligand of numb-protein X 1	Putatively involved in neuregulin-1/ErbB signaling	
D	Plcd1	Phospholipase C, delta 1	PKC signaling molecule involved in ischemic heart response	Mm.23963
d[d,d]	Slit2	Slit homolog 2	Secreted negative regulator of axonal extension	Mm.289739
D[b]	Vsnl1	Visinin-like 1	Calcium binding protein; unknown biological function	Mm.27005
D	Wisp1	WNT1 inducible signaling pathway protein 1	Wnt signaling pathway; potential growth factor	Mm.10222
u	Bsf3	Cardiotrophin-like cytokine factor 1	Cytokine involved in Jak/STAT signaling	Mm.347919
u	Oprl1	Kappa3-related opioid receptor isoform E	G-protein coupled receptor	Mm.285075
u	Tslpr	Thymic stromal-derived lymphopoietin, receptor	Cytokine receptor	Mm.35771
Transcription and transcriptional regulation				
D[b]	Brd8	Bromodomain containing 8	Transcription factor; nuclear coactivator of aRxr	Mm.45602
D	Ddit3	DNA damage-inducible transcript 3	Transcription factor involved in stress-mediated apoptosis	Mm.110220
D	Eya1	Eyes absent 1 homolog (*Drosophila*)	Transcription factor; implicated in Caylor cardiofacial syndrome	Mm.250185
D[b,d]	Hand1	Heart and neural crest derivatives expressed transcript 1	Transcription factor/expressed in left ventricle	Mm.4746
d[a]	Hcfc1	Host cell factor C1	Transcriptional coregulator; part of HDAC DNA methylation/demethylation complex	Mm.248353
d	Hrmt1l1	Heterogeneous nuclear ribonucleoprotein methyltransferase-like 1	*S*-adenosylmethionine-dependent methyltransferase activity; may be involved in regulation of transcription	Mm.32020
D[b,d]	Irx2	Iroquois-related homeobox 2 (*Drosophila*)	Transcription factor/expressed in IVS	Mm.28888
D	LOC433393	Weakly similar to diaphanous protein homolog 1	Putative TATA-box binding protein; unknown biological function	Mm.331444
D[a]	Nolz1	Zinc finger protein 503	Putative transcription factor	Mm.292401
D	Rbed1	RNA binding motif and ELMO domain 1	Nucleic acid binding protein; unknown biological function	Mm.24440l
D[b,d]	Shox2	Short stature homeobox 2	Transcription factor/expressed in developing vena cava	Mm.39093
D[b]	Tbx3	T-box transcription factor 3	Transcription factor/expressed in developing conduction system	Mm.87711
D	Tia1	Cytotoxic granule-associated RNA binding protein 1	Translational silencer; RNA-binding protein	Mm.274425
d[a,b]	Yap1	Yes-associated protein	WW domain containing transcriptional coactivator	Mm.221992
U[a]	Ddx52	DEAD (Asp-Glu-Ala-Asp) box polypeptide 52	Putative helicase activity	Mm.280544
u	HoxB7	Homeobox B7	Hox-cluster transcription factor	Mm.4822
Known genes and ESTs with unknown function				
d	1110033J19	RIKEN cDNA 1110033J19 gene	Unknown biological function	Mm.3572
D[a]	1300012G16	RIKEN cDNA 1300012G16 gene	Unknown biological function	Mm.100065
D	1810015C04	RIKEN cDNA 1810015C04 gene	Unknown biological function	Mm.25311
D	2210403K04	RIKEN cDNA 2210403K04 gene	Unknown biological function	Mm.41393
D	2610024A01	RIKEN cDNA 2610024A01 gene	Unknown biological function	Mm.281287
d	2610318I15	RIKEN cDNA 2610318I15 gene	Unknown biological function	Mm.262707

Table 2 (*continued*)

Up/down[A]	Gene symbol	Gene title	Proposed biological functions	Unigene code
Known genes and ESTs with unknown function				
D	4921517N04	Riken cDNA 4921517N04 gene	Unknown biological function	Mm.276415
D	4933417N17	Hypothetical protein 4933417N17	Unknown biological function	Mm.72979
D[a]	4933428I03	RIKEN cDNA 4933428I03 gene	Unknown biological function	Mm.254605
D	5730508B09	RIKEN cDNA 5730508B09 gene	Unknown biological function	Mm.317049
d	BC031781	cDNA sequence BC031781	Unknown biological function	Mm.272625
D	C230093N12	RIKEN cDNA C230093N12 gene	Unknown biological function	Mm.4065
D	Copg2as2	Coatomer protein complex, subunit gamma 2, antisense 2	Antisense of the imprinted gene Copg2; Unknown biological function	Mm.22891
D	D12Ertd553e	D12Ertd553e	Unknown biological function	Mm.275699
D	E130311K13	Hypothetical protein E130311K13	Unknown biological function	Mm.39342
D	LOC432731	Similar to zinc finger protein 187	Unknown biological function	Mm.235360
D	mKIAA1961	mKIAA1961 protein	Unknown biological function	Mm.34087
d	Mtcp1	Mature T-cell proliferation 1	Gene expressed in T-cell leukemias; Unknown biological function	Mm.16366
d	Trim5	Tripartite motif protein 5	Unknown biological function	Mm.259010
u	0610009K11	RIKEN cDNA 0610009K11 gene	Unknown biological function	Mm.103413
U	2010308M01	RIKEN cDNA 2010308M01 gene	Unknown biological function	Mm.371646
u[a]	2810487N22	RIKEN cDNA 2810487N22 gene	Unknown biological function	
U	4122402O22	RIKEN cDNA 4122402O22 gene	Unknown biological function	Mm.34659
U	4930429A08	RIKEN cDNA 4930429A08 gene	Unknown biological function	Mm.172064
u	4930461P20	RIKEN cDNA 4930461P20 gene	Unknown biological function	Mm.297862
U	A230046K03	RIKEN cDNA A230046K03 gene	Unknown biological function	Mm.278577
u[a]	AI413631	cDNA sequence AI413631	Unknown biological function	Mm.310434
u[a]	Bola3	bolA-like 3	Unknown biological function	Mm.52024
U[a]	Chchd6	Coiled-coil-helix-coiled-coil-helix domain containing 6	Unknown biological function	Mm.20313
U	Pqlc3	PQ loop repeat containing 3	Unknown biological function	Mm.5675
u	Stom	Stomatin	Unknown biological function	Mm.295284
U	Trim47	Tripartite motif protein 47	Unknown biological function	Mm.5510
u	Trim62	Tripartite motif-containing 62	Unknown biological function	Mm.30653

U/*D*, significantly upregulated or downregulated, respectively, with expression change $\log_2 > \pm 0.3$. u/d, significantly upregulated or downregulated respectively with expression change $\log_2 < \pm 0.3$. Note that upregulation or downregulation of gene expression was based on Tbx5del/+ relative to WT.

[a] Conflicting direction of expression changes between Tbx5lox/+ and Tbx5del/+ data (i.e., expression significantly down in Tbx5lox/+ but significantly up in Tbx5 del/+ or visa versa, perhaps due to secondary compensatory responses).

[b] Confirmed by either in situ hybridization or real-time PCR as having a significant expression change consistent with the microarray data.

[c] In situ hybridization or real-time PCR was not able to confirm a significant expression change as reported in the array.

[d] *P* values (del/+ vs. WT) between 5% and 10%.

showed altered expression consistent with the microarray data (Fig. 7A; Supplemental Figure 2). Additionally, we also quantitated expression of the transcription factors *Hand1*, *Shox2*, *Irx2*, and *Irx1*—expressed in an overlapping domain with *Irx2* in the intraventricular septum (Christoffels et al., 2000) and found all were significantly decreased in $Tbx5^{del/+}$ and $Tbx5^{lox/+}$ hearts. *Tbx2*, expressed in an overlapping pattern with *Tbx3* in the atrioventricular canal (Gibson-Brown et al., 1998; Habets et al., 2002; Yamada et al., 2000), was not increased in mutant hearts (Supplemental Figure 2). Expression of *Myl2* and *Irx4* (genes known to be downregulated exclusively in $Tbx5^{del/del}$ embryos) were used as negative controls and showed no statistically significant changes in expression in either heterozygous mutant. In total, we independently confirmed expression changes in 17 of 23 genes (74%) consistent with the changes reported by the microarray screen.

When changes in gene expression (δx) were examined as a function of *Tbx5* mRNA levels (δd), several different expression kinetics were observed, most likely indicative of varying modes of gene regulation (Figs. 7B–J). At one extreme, $\delta x/\delta d$ for *Gja5* expression remained constant at all *Tbx5* levels examined ($R^2 = 0.77$), as reflected by the linear relationship between *Tbx5* dosage and *Gja5* expression. In comparison, the $\delta x/\delta d$ of *Vsnl1*, *Shox2*, and *Ddc* was constant at concentrations of Tbx5 near 100% but rapidly changed at lower *Tbx5* dosages, consistent with a prompt loss in either gene activation (*Vsnl1*, *Shox2*) or in gene repression (*Ddc*). *Tbx3* exhibited the most dynamic changes in expression, best described by a sinusoidal curve ($R^2 = 0.73$) such that the $\delta x/\delta d$ was constant at high and low concentrations of *Tbx5* but changed rapidly between 50% and 90% WT *Tbx5* mRNA levels, consistent with a threshold-mediated method of gene expression control. Examination of *Irx4* (Fig. 5G; $R^2 = 0.007$) or *Myl2* ($R^2 = 0.003$) expression showed no obvious change in the general level of expression of with decreasing *Tbx5* dosage within the range of *Tbx5* mRNA levels examined ($\delta x/\delta d \approx 0$).

Of the 16 genes examined in $Tbx5^{lox/+}$, 6 showed greater expression changes in hypomorphic samples than in $Tbx5^{del/+}$ hearts, albeit in only one case (*Brd8*) was this difference statistically significant ($P < 0.0001$). By plotting the expression of these genes, more complex interactions were observed. For instance, *Brd8* expression was increased in $Tbx5^{del/+}$ hearts

Table 3
Moderately sensitive *Tbx5* downstream genes (only altered in *Tbx5*$^{del/+}$)

Up/down[A]	Gene symbol	Gene title	Proposed biological functions	Unigene code
Cell cycle				
u	Orc1l	Origin recognition complex, subunit 1-like	Involved in DNA replication initiation	Mm.294154
U	S100a6	S100 calcium binding protein A6 (calcyclin)	Cation sensing protein involved in cell cycle regulation	Mm.100144
Channel Forming				
U	Kctd10	Potassium channel tetramerization domain containing 10	Ion channel; unknown biological function	Mm.268504
u	Nupl1	Nucleoporin like 1	Nuclear pore complex	Mm.258051
Cellular/structural component				
d	Myl7	Myosin, light polypeptide 7, regulatory	Cytoskeletal component	Mm.46514
D	Nup214	Nucleoporin 214	Part of nuclear pore complex	Mm.127697
d	Phlda1	Pleckstrin homology-like domain, family A, member 1	FasL-mediated induction of apoptosis	Mm.3117
d	Rpl28	Ribosomal protein L28	Ribosomal structural protein	Mm.379002
d	Rpl4	Ribosomal protein L4	Ribosomal structural protein	Mm.280083
d	Tspan5	Tetraspanin 5	Transmembrane protein; unknown biological function	Mm.31927
U	Tnni2	Troponin I, skeletal, fast 2	Calcium transporter involved in muscle contraction	Mm.39469
Kinase				
d	Cerk	Ceramide kinase	Ceramide phosphorylation; mediator of apoptosis pathway	Mm.222685
D	Hk1	Hexokinase 1	Hexokinase; unknown biological function	Mm.213213
D	Prkab1	Protein kinase, AMP-activated, beta 1 non-catalytic subunit	AMP-activated protein kinase; unknown biological function	Mm.200912
U	Ltb4dh	Leukotriene B4 12-hydroxydehydrogenase	Alcohol dehydrogenase; unknown biological function	Mm.34497
u	Prkar2b	Protein kinase, cAMP-dependent regulatory, type II beta	Regulatory subunit of cAMP-kinases	Mm.25594
U	Riok2	RIO kinase 2	Kinase; unknown biological function	Mm.218423
Metabolism and biosynthesis				
d	Asph	Aspartate-beta-hydroxylase	Peptide-aspartate beta-dioxygenase activity; unknown biological activity	Mm.239247
d	Entpd5	Ectonucleoside triphosphate diphosphohydrolase 5	Extracellular NTP-ase activity; unknown biological activity	Mm.10211
d	Ercc1	Excision repair cross-complementing rodent repair deficiency, complementation group 1	DNA damage repair	Mm.280913
D	Lap3	Leucine aminopeptidase 3	Aminopeptidase; unknown biological function	Mm.341797
d	Lrrc41	Leucine-rich repeat containing 41	Ubiquitin ligase	Mm.260786
d	Nudt13	Nudix (nucleoside diphosphate linked moiety X)-type motif 13	Hydrolase activity; unknown biological activity	Mm.317636
D	Sulf2	Sulfatase 2	Sulfuric ester hydrolase; unknown biological function	Mm.280459
u	Adss2	Adenylosuccinate synthetase 2, non-muscle	Adenylosuccinate synthase activity; unknown biological activity	Mm.338021
u	Agpat3	1-Acylglycerol-3-phosphate *O*-acyltransferase 3	Acyltransferase activity; phospholipid biosynthesis	Mm.141230
U	Bdh	3-Hydroxybutyrate dehydrogenase (heart, mitochondrial)	Oxidoreductase; unknown function	Mm.293470
U	Gpt2	Glutamic pyruvate transaminase (alanine aminotransferase) 2	Transaminase; unknown biological function	Mm.200423
u	Rad51c	Rad51 homolog c	DNA damage repair	Mm.37376
U	Spi6	Serine (or cysteine) proteinase inhibitor, clade B, member 9	Peptidase involved in immune response	Mm.3368
Metabolite transport				
d	Cpne5	Copine V	Calcium-dependent phospholipid-binding protein; putative molecular chaperone	Mm.39905
d	Dnajb12	DnaJ (Hsp40) homolog, subfamily B, member 12	Molecular chaperone	Mm.103610
D	Doc2g	Double C2, gamma	Vesicular transport	Mm.266972
d	Kpnb3	Karyopherin (importin) beta 3	Nuclear import protein	Mm.221452
u	Kpna3	Karyopherin (importin) alpha 3	Nuclear import protein	Mm.25548

Table 3 (*continued*)

Up/down[A]	Gene symbol	Gene title	Proposed biological functions	Unigene code
Signal transduction				
D	Braf	Braf transforming gene	Protein involved in extracellular signal-regulated kinase (ERK) signaling	Mm.245513
d	Capn6	Calpain 6	Calcium-dependent cysteine protease; unknown biological function	Mm.30290
D	Gnb3	Guanine nucleotide binding protein, beta 3	G-protein-coupled receptor; unknown biological function	Mm.68889
D	Pak2	P21 (CDKN1A)-activated kinase	Role in non-Smad Tgf-beta signaling	Mm.234204
d	Sema4d	Semaphorin 4D	Secreted negative regulator of axonal extension	Mm.33903
u	Arl6	ADP ribosylation factor-like 6	GTPase signal transduction	Mm.7760
U	Sema6a	Semaphorin 6A	Transmembrane negative regulator of axonal extension	Mm.40909
Transcription and transcriptional regulation				
d	Ascc1	Activating signal cointegrator 1 complex subunit 1	Transcriptional coactivator	Mm.155839
D[a]	Cited1	Cbp/p300-interacting transactivator with Glu/Asp-rich carboxy-terminal domain 1	Transcription factor/expressed dynamically in the heart	Mm.2390
D	E4f1	E4F transcription factor 1	Transcription factor which is also needed for mitosis	Mm.163132
D	Eif4g1	Eukaryotic translation initiation factor 4, gamma 1	Transcription initiation factor	Mm.260256
d	Fhl2	Four and a half LIM domains 2	Muscle-restricted transcriptional coactivator; expressed in heart	Mm.6799
d	Foxk2	Forkhead box K2	Transcription factor; unknown biological function	Mm.209750
D	Gli2	GLI-Kruppel family member GLI2	Transcription factor; Shh signal transduction	Mm.273292
d	Thoc2	THO complex 2	Transcriptional elongation and mRNA export factor	Mm.259498
d[b]	Taz	WW domain containing transcription regulator 1	(W) domain containing positive transcriptional coregulator; expressed in the heart	Mm.227202
d	Zbtb9	Zinc finger and BTB domain containing 9	Transcription factor; unknown biological function	Mm.328890
D	Zfp207	zinc finger protein 207	Transcription factor	Mm.102253
U	Ddx54	DEAD (Asp-Glu-Ala-Asp) box polypeptide 54	Putative transcription factor; helicase activity	Mm.62044
U	Hmgb1	High mobility group box 1	DNA-binding protein; potential cytokine	Mm.207047
U[a]	Syncrip	Synaptotagmin binding, cytoplasmic RNA interacting protein	mRNA stabilization	Mm.260545
Known genes and ESTs with unknown function				
D	0610037L13	RIKEN cDNA 0610037L13 gene	Unknown biological function	Mm.274853
D	1498131	Mus musculus, clone IMAGE:1498131, mRNA	Unknown biological function	Mm.374459
d	1810007M14	RIKEN cDNA 1810007M14 gene	Unknown biological function	Mm.347
d	2310009B15	RIKEN cDNA 2310009B15 gene	Unknown biological function	Mm.264673
d	2410029D17	RIKEN cDNA 2410029D17 gene	Unknown biological function	N/A
d	2610204M12	RIKEN cDNA 2610204M12 gene	Unknown biological function	Mm.361788
D	4833427F10	RIKEN cDNA 4833427F10 gene	Unknown biological function	Mm.290828
D	4930565B19	RIKEN cDNA 4930565B19 gene	Unknown biological function	Mm.28804
d	4933439C20	RIKEN cDNA 4933439C20 gene	Unknown biological function	Mm.335641
d	6430550H21	RIKEN cDNA 6430550H21 gene	Unknown biological function	Mm.383286
d	Adprhl2	ADP ribosylhydrolase like 2	Unknown biological function	Mm.11285
D	BC031361	cDNA sequence BC031361	Unknown biological function	Mm.359954
D	C130052G03	RIKEN cDNA C130052G03 gene	Unknown biological function	Mm.276075
d	Mest	Molossinus mesoderm-specific transcript	Unknown biological function	Mm.335639
d	MGC38812	Hypothetical protein MGC38812	Unknown biological function	Mm.206371
d	Pqlc1	PQ loop repeat containing 1	Unknown biological activity	Mm.29247
u	0610010O12	RIKEN cDNA 0610010O12 gene	Unknown biological function	Mm.272527
u	1700027J05	RIKEN cDNA 1700027J05 gene	Unknown biological function	Mm.383229
U	3632431M01	Transmembrane and coiled coil domains 1	Unknown biological function	Mm.333338
U	4921529O18	RIKEN cDNA 4921529O18 gene	Unknown biological function	Mm.266280
u	AV214133	cDNA sequence AV214133	Unknown biological function	
U	BC023488	cDNA sequence BC023488	Unknown biological function	Mm.209490
u	BI134269	cDNA sequence BI134269	Unknown biological function	Mm.339029
U	C330027C09	RIKEN cDNA C330027C09 gene	Unknown biological function	Mm.24491
u	Rga	Recombination activating gene 1 gene activation	Unknown biological function; membrane protein	Mm.17958
u	Tmepai	Transmembrane, prostate androgen-induced RNA	Unknown biological function; membrane protein	Mm.73682

U/*D*, significantly upregulated or downregulated respectively with expression change $\log_2 > \pm 0.3$. u/d, significantly upregulated or downregulated respectively with expression change $\log_2 < \pm 0.3$. Note that upregulation or downregulation of gene expression was based on Tbx5del/+ relative to WT.

[a] In situ hybridization or real-time PCR was not able to confirm a significant expression change as reported in the array.

[b] Confirmed by either in situ hybridization or real-time PCR as having a significant expression change consistent with the microarray data.

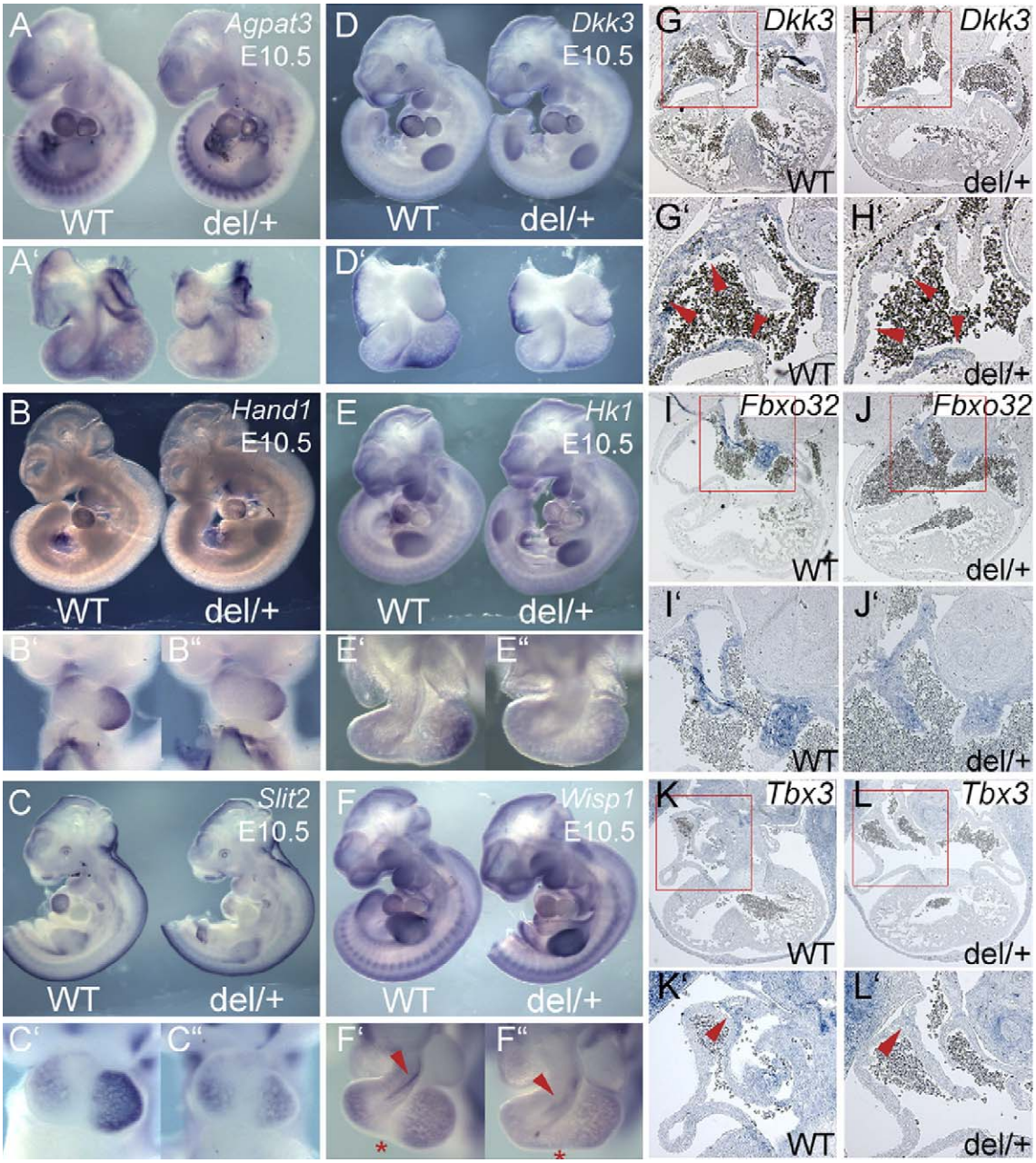

Fig. 6. Whole-mount and section in situ hybridization (performed at E10.5 and E11.5, respectively) examining expression of 8 genes identified on the microarray revealing significant changes in expression consistent with microarray data. *Agpat3* (A, A′), *Hand1* (B–B″), *Slit2* (C–C″), *Dkk3* (D, D′, G, G′ H, H″), *Hk1* (E–E″), *Wisp1* (F–F″), *Fbxo32* (I, I′, J, J′) and *Tbx3* (K, K′, L, L′) all show downregulation by in situ. In addition, *Wisp1* expression is expanded through the interventricular septum (see * in F′ and F″). Squares in panels G–L show those regions that are magnified in panels G′–L′).

while it was decreased in $Tbx5^{lox/+}$ hearts leading to an inverted bell-shaped curve. In contrast, *Cdo1* expression could not be described by a trend line but rather appeared to separate into two distinct clusters, one higher than another. Cardiac expression of *Fbxo32* showed a clearly linear relationship in wild-type and $Tbx5^{lox/+}$ samples and in a subset of $Tbx5^{del/+}$ hearts. However, at the lower extreme, some heterozygous null hearts begin expressing more *Fbxo32*.

An important caveat of these analyses is that difference in gene expression measured from whole E12.5 hearts may not reflect dynamic spatiotemporal changes in gene expression, such as the decreased but expanded expression of *Nppa*, and

Fig. 7. Quantitative real-time PCR analysis of gene expression. (A) Average changes in gene expression of 16 genes shown to have altered expression in $Tbx5^{del/+}$ hearts by microarray analysis; *$P < 0.05$. *Irx4* and *Myl2* are negative controls. (B–J) Profiles of gene expression in individual hearts in relation to *Tbx5* mRNA levels reveal different kinetic interactions from linear (*Gja5*) to sinusoidal (*Tbx3*). The expression of genes such as *Cdo1* and *Fbxo32* appear to be differentially expressed within individual hearts of the same genotype, suggesting that compensatory mechanisms might be adjusting gene expression to try and compensate for the loss of *Tbx5*. 100% is defined as the average of wild type on both axes.

furthermore, changes in distinct regions of the heart might be masked by the absence of change elsewhere in the heart. It is also possible that the differential expression of some genes may be reflective of decreased growth or failed differentiation of certain cardiac structures, which cannot be assessed by measuring gene expression. Therefore, these 182 gene clusters

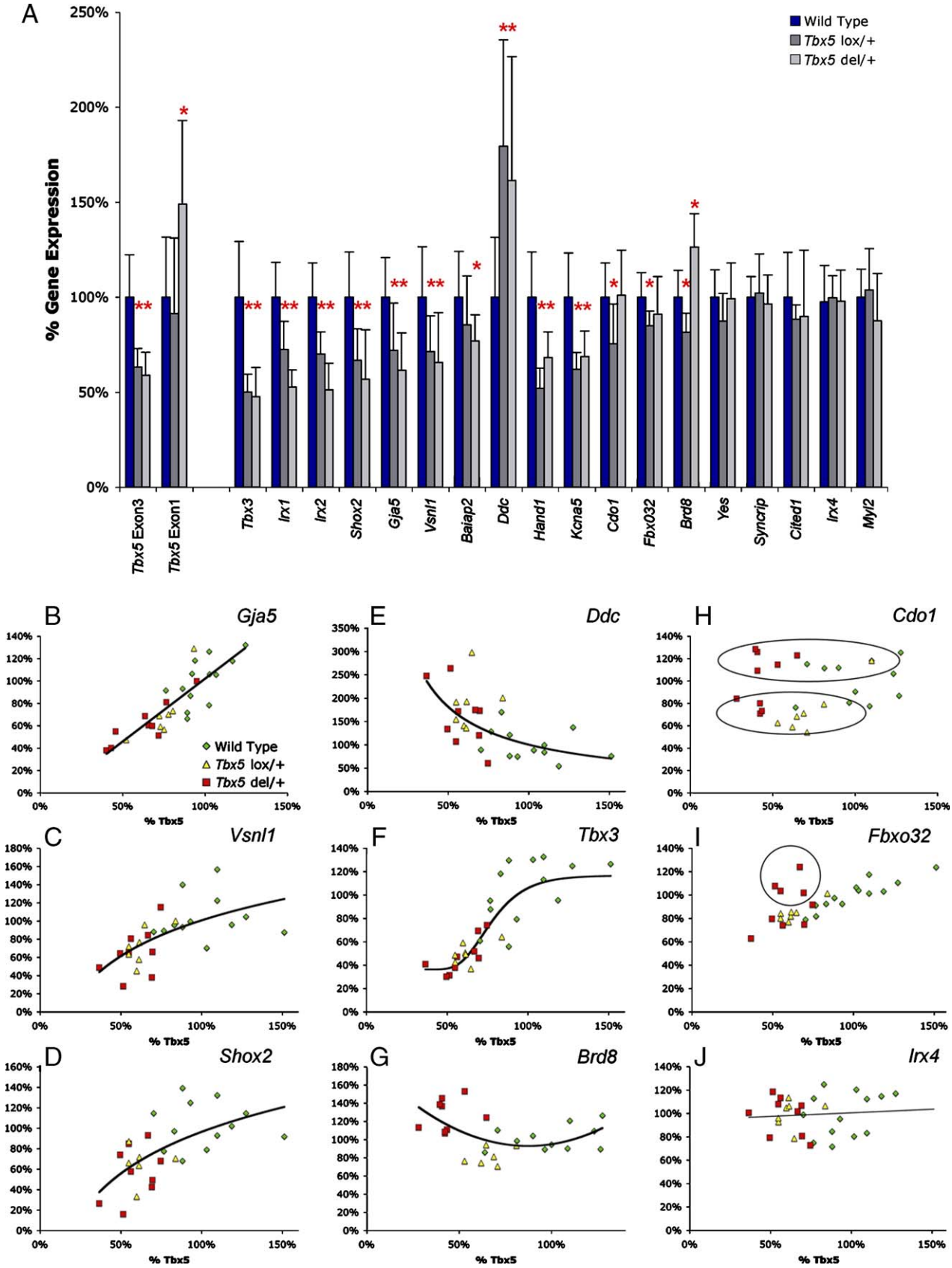

do not represent an exhaustive list of *Tbx5*-regulated genes but rather are a subset of *Tbx5* dosage-sensitive genes, some of which may be causative in the etiology of HOS. Nonetheless, it is clear that dosage of Tbx5 is key to regulation of several genes in complex and dynamic patterns.

Tbx5 binding site clusters in dosage-sensitive genes

Tbx5 binds a consensus DNA sequence loosely defined as A/G/TG/AGTGNNA. Using a position weight matrix (PWM) based on all published T-box binding sites (Fig. 8A), an in silico

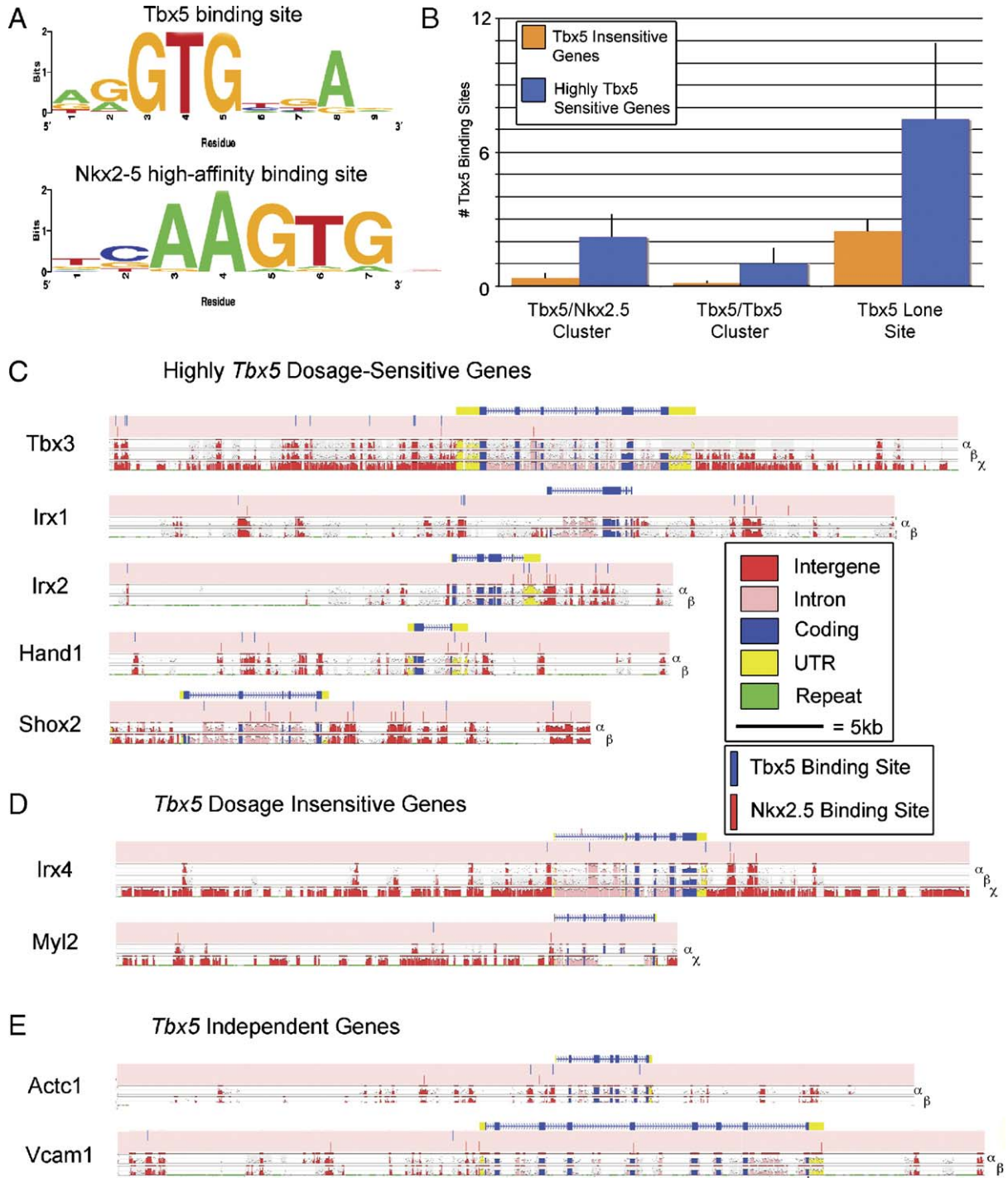

Fig. 8. Frequency and positioning of T-box and Nkx2.5 transcription factor binding sites surrounding *Tbx5*-sensitive genes. (A) High-quality position weight matrices for T-box binding sites (TBEs) and Nkx2.5 binding sites (NBEs) were used to define transcription factor binding sites. (B) The frequency of TBEs either alone or as clustered sites tends to increase in the genomic region surrounding *Tbx5* dosage-sensitive targets (±standard error). (C–E) Genomic positioning of TBEs and TBE/NKE clusters on DNA surrounding both *Tbx5*-sensitive genes (C), and *Tbx5*-insensitive (D) and *Tbx5*-independent genes (E) appear dispersed both up- and downstream and within intronic regions, suggesting that TBE position by itself is not predictive of *Tbx5* dosage sensitivity. Alignments were performed between mouse and dog (α), mouse and human (β), and mouse and rat (δ).

analysis of potential genomic regulatory regions, both around and within the validated set of *Tbx5* dosage-sensitive genes, was performed using MULAN and MultiTF to examine the frequency and position of evolutionarily conserved T-box binding elements (TBEs) between mouse, human, rat, and dog. In addition, as synergy with Nkx2-5 may be a key mechanism for dosage sensitivity, a similar analysis was performed to identify Nkx2.5 binding sites (NBEs) using the PWM shown in Fig. 8A. A set of 9 myocardial genes insensitive to *Tbx5* dosage (defined as not altered on the $Tbx5^{del/+}$ microarray) were used as a control set to determine the baseline frequency of randomly positioned TBEs/NBEs within a given genomic region.

The positioning of lone TBEs or TBE/NBE clusters within the DNA surrounding dosage-sensitive targets reveals no obvious spatial similarities between genes (Fig. 8C). Transcription factor binding sites surrounding *Tbx3*, as an example, are located exclusively upstream of the gene and consist of numerous TBEs and two clustered sites separated by greater than 15 kb. In contrast, DNA binding sites near *Irx2* are almost exclusively located within the 3′ UTR and downstream genomic region where several clustered sites appear to be tightly grouped. *Irx1* and *Hand1*, in comparison, have both up- and downstream clustered sites, whereas *Shox2* has numerous dispersed sites within intronic DNA. Similarly, when transcription factor binding sites were examined in the set of *Tbx5*-insensitive/independent genes (Figs. 8D and E), no obvious pattern in binding site position was noted, although the number of sites (both lone and clustered sites) did seem to decrease (see below). This analysis suggests that the positional location of TBEs and NBEs is not predictive of a gene's sensitivity to *Tbx5* dosage. It should be noted, however, that this search is not exhaustive of all possible Tbx5 interactions (Tbx5 has been shown to physically interact and synergize with GATA4 for example; Garg et al., 2003) and is limited to the examination of only 25 kb upstream and 15 kb downstream surrounding the genes of interest.

The number of TBEs and clustered TBE/NKE sites were quantitated in both our highly sensitive (n = 17) and non-sensitive (n = 9) group of genes (Fig. 8B). Keeping in mind that it is unlikely that all 17 analyzed *Tbx5*-sensitive genes are direct Tbx5 targets, our analysis reveals that *Tbx5*-sensitive genes have a trend towards having greater numbers of TBEs within the genomic region flanking them than genes in the non-sensitive control group (7.4 ± 3.4 vs. 2.4 ± 0.5). In addition, the number of clustered TBE/TBE and TBE/NKE sites also tends to be higher in the sensitive population (1.0 ± 0.7SE vs. 0.1 ± 0.1SE and 2.2 ± 1.0SE vs.0.3 ± 0.2SE, respectively). Therefore, increased TBE density, either alone or in close association with Nkx2.5 sites, may be a potential indicator of *Tbx5* dosage sensitivity.

Discussion

We have shown, using a *Tbx5* allelic series, that the developing mouse heart is exquisitely sensitive to altered dosage of *Tbx5* (summarized in Table 1). By gene expression profiling, we have uncovered subsets of genes downstream of *Tbx5* that may be involved in regulating CHD severity due to *Tbx5* haploinsufficiency. The rheostatic regulation of cardiac gene expression by *Tbx5* indicates that the variable expressivity of *TBX5* mutations in humans is likely to be due to threshold regulation of differentially sensitive genes.

Tbx5 dosage and cardiac morphogenesis

We observed a very close correlation between *Tbx5* dosage and the severity of defective cardiac morphogenesis. Hypomorphic heterozygous mice ($Tbx5^{lox/+}$) consistently had milder conduction system disease and a concurrent dramatic increase in survivability over the heterozygous null mice. Likewise, homozygous hypomorphs ($Tbx5^{lox/lox}$) had better developed cardiac structures and survived one day longer than $Tbx5^{del/del}$ null embryos. These results illustrate that even slight differences in *Tbx5* dosage (of <15%) during development can lead to dramatic changes in phenotype.

In examining the differences observed between *Tbx5* hypomorphic and null mutants, we observed a large initial disparity in *Tbx5* dosage between heterozygous mutants. Interestingly, this difference was observed at E8.5, at a time when *Tbx5* is expressed as an anterior–posterior gradient in the linear heart tube with strongest expression in posterior regions destined to become atria (Bruneau et al., 1999). Furthermore, it has been suggested that *Tbx5* might bind its own promoter and induce its own expression in vitro (Sun et al., 2004). If *Tbx5* does regulate its own expression in vivo, small differences in initial *Tbx5* dosage due to haploinsufficiency may result in delayed establishment of this anterior–posterior event, thus postponing or precluding crucial patterning or differentiation events within the heart.

Differential sensitivity of downstream genes to the Tbx5 dosage gradient

Increased severity of CHDs due to decreased *Tbx5* levels correlated with critical changes in gene expression, and translated to altered survival. It is likely that genes that are highly sensitive to perturbations in *Tbx5* levels are associated with fundamental disease-associated processes, whereas those that are only moderately affected by *Tbx5* haploinsufficiency perhaps have roles in modulating the severity of the HOS-associated defects. In human populations, this might be reflected in the large variation that exists in families with HOS or other CHDs. Modifier genes might therefore be involved in modulating *Tbx5* expression from the remaining wild-type allele in response to haploinsufficiency or may act as genetic amplifiers to enhance expression of specific *Tbx5* targets.

Dynamics of gene regulation by Tbx5

Examination of expression dynamics for genes regulated by Tbx5 illustrates distinctly different responses to decreasing

Tbx5 dosage. The expression of a subset of genes can be defined as a direct function of the dosage of *Tbx5* as would be expected if they represent direct Tbx5 targets, as has been shown for *Gja5* (Bruneau et al., 2001). In contrast, expression of other genes can change rapidly at lower levels of Tbx5, and in some cases gene expression changes were observed to exhibit stochastic expression properties. The regulatory modules that control the Tbx5 responsiveness of the former subset of downstream genes must be regulated by more complex interactions between Tbx5 and other positively or negatively acting transcription factors, whereas the latter group appear only *Tbx5* dose-responsive in a subset of the same genotype, most likely due to the action of additional genetic modifiers that might independently adjust gene expression to compensate for the loss of *Tbx5*. Deciphering the nature of these dynamic transcriptional rheostats in model organisms has to date yielded conflicting information, and thus will be difficult to resolve. Together these data indicate that Tbx5 can regulate downstream genes via an array of independent mechanisms, some of which will include direct DNA binding, and others via indirect mechanisms that may involve complex regulatory networks.

Tbx5 regulates transcription factor networks in the heart

Several of the genes identified by gene expression profiling are transcription factors or are involved in transcriptional regulation, which places Tbx5 upstream of numerous different transcriptional cascades in the developing heart. For example, the transcriptional repressor *Tbx3* is significantly reduced in the *Tbx5* mutant hearts. *Tbx3* cardiac expression is seen from E8.5 onward in the myocardium that will become cardiac conduction system and is maintained throughout development in the sinoatrial and atrioventricular nodes as well as in the cardiac bundle branches (Hoogaars et al., 2004). Tbx5 and Tbx3 compete for binding sites on the promoters of *Gja5* and *Nppa* (two direct targets activated by *Tbx5*) in dosage-dependent manners (Hoogaars et al., 2004). Our results suggest that *Tbx5* normally enhances *Tbx3* expression, thus creating a regulatory feedback circuit whereby *Tbx5* sustains the expression of *Tbx3*, which in turn locally counters the activation of certain genes by *Tbx5* within the cardiac conduction system (Fig. 9). That the regulation of *Tbx3* is sensitive to Tbx5 dosage allows for the creation of sharp boundaries of expression upon reaching a given dosage of Tbx5 thus ensuring the correct balance between activator (Tbx5) and repressor (Tbx3) is maintained. This reveals a crucial and very fine genetic interaction between T-box transcription factors in the developing heart, which has evolved very specifically to preserve accurate spatiotemporal transcription of cardiac genes even in the face of genetic disturbances. The architecture of such a genetic feedback loop where transactivator and transrepressor compete for binding to common DNA binding sites has been shown to induce rapid dosage-dependent switching behaviour in gene expression in vitro (Rossi et al., 2000).

The transcriptional coactivators *Yap1* and *Taz* are also both downregulated in *Tbx5* mutant mice. It has been shown recently that both Yap1 and Taz interact as part of the Tbx5 transcriptional machinery to potently promote Tbx5-dependent transcription (Murakami et al., 2005). It has been suggested that this coactivation may occur through interactions between Taz and histone acetyltransferases (HATs) (Murakami et al., 2005). It is possible therefore that the differential sensitivity of downstream genes to *Tbx5* dosage is due in part to varying degrees of histone modification of Tbx5 target gene promoter sequences. Minor perturbations in the level of *Tbx5*, combined with further decreases in the expression of both *Taz* and *Yap1* would render genes in highly deacetylated regions of chromatin less accessible to Tbx5 activation, whereas genes situated less condensed regions of chromatin would be less sensitive to decreased HAT recruitment and would therefore remain transcriptionally active.

In addition to disrupting transcriptional networks, *Tbx5* haploinsufficiency also alters numerous signaling cascades in the developing heart. The secreted signaling molecule *Slit2* that we show to be predominantly expressed in ventricular trabeculae is also downstream of *Tbx5* in the heart. Slit2,

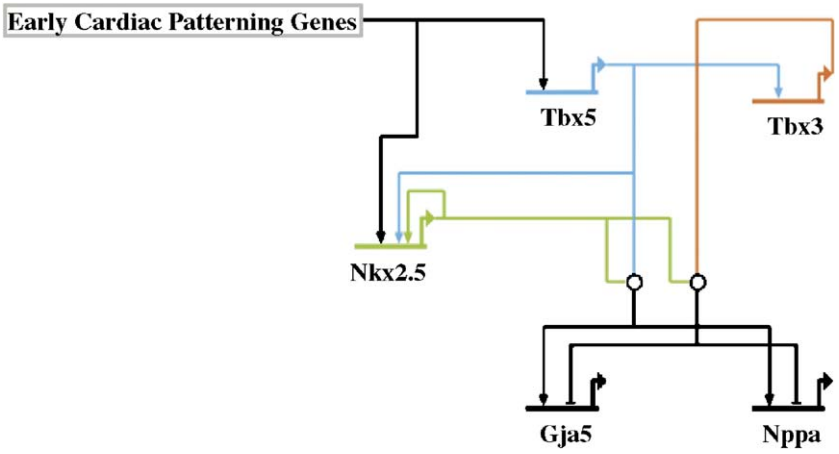

Fig. 9. This gene regulatory network is implied by microarray and real-time data wherein the regulation of *Gja5* and *Nppa* occur via interactions between Tbx5 and Tbx3 with Nkx2.5.

originally identified as a repulsive cue during axonal pathfinding, has also been shown to act as a potent chemorepellant during cell migration (Wu et al., 2001). Additionally, *Drosophila slit* has recently been shown to act as a guide to align myocardial cells converging at the midline during heart tube closure in fly (Qian et al., 2005). The expression of *Slit2* on either side of the interventricular septum may form a repulsive corridor that might help position the location of septal outgrowth.

Tbx5 mutant mice also show disruptions in the expression of genes involved in inhibition of the Wnt/β-catenin signaling pathway (*Cxxc4*, *Dkk3*). The balance between Wnts and their antagonists play a critical role in shaping the primary heart field during early cardiogenesis. Wnt/β-catenin signals emanating from the neural tube act as negative regulators of myocardial cell fate (Marvin et al., 2001; Tzahor and Lassar, 2001). Wnt antagonists counterbalance these inhibitory signals and have been shown to play important roles in promoting cardiac mesoderm formation (Lickert et al., 2002; Marvin et al., 2001; Tzahor and Lassar, 2001). Decreases in *Cxxc4* and *Dkk3* in *Tbx5*-deficient mice most likely would disrupt proper cell fate specification during heart development. Decreases in *Gsk3*β (involved in the Wnt-induced production of β-catenin) may partially compensate for loss of these important Wnt inhibitors while accounting for downregulation of *Wisp1* (normally induced by Wnt1/β-catenin expression; Xu et al., 2000). Expanded *Wisp1* expression across the interventricular septum is also consistent with disrupted cellular specification.

T-box genes have been shown in vivo to interact in regulatory networks to carefully pattern specific tissues through synergistic and antagonistic interactions with other transcription factors (including but not restricted to other T-box transcription factors) in fish, worm, and mice (Goering et al., 2003; Koshiba-Takeuchi et al., 2006; Pocock et al., 2004; Takeuchi et al., 2005). Such regulatory networks of transcription factors ensure specificity of patterning and very fine regulation of output levels but also open up a large network to perturbed levels of the primary regulator, in this case Tbx5.

Conclusions

The dosage of *Tbx5* communicates spatiotemporal information to cells within the early heart that is used to carefully orchestrate patterns of cardiac development and it is well established that decreases in *Tbx5* dosage cause congenital heart defects. We have shown that there is a direct relationship between *Tbx5* dosage during early heart development and the severity of concomitant heart defects. It is likely that such differences in *Tbx5* dosage brought about due to slightly different genetic backgrounds and the effect of modifier genes account for the large variation in severity of HOS clinical presentation. Changes in the severity of CHDs are underpinned by differential sensitivities of downstream genes to varying levels of *Tbx5*. These differences represent variation in the underlying control elements that regulate the expression of these genes and are important to investigate as changes in these genes lead to a marked increase in survivability.

Acknowledgments

We would like to acknowledge John Wylie for technical assistance and Dr. Elisabeth Tillier for intellectual discussions. This work was supported by grants to B.G.B. from the March of Dimes Birth Defects Foundation (1-FY05-117), the Canadian Institutes of Health Research, the Heart and Stroke Foundation of Ontario (HSFO), as well as support from the Howard Hughes Medical Institutes (J.G.S, C.E.S.), the Canada Foundation for Innovation (R.M.H.), an HSFO John D. Schultz summer studentship (I.V.), a Natural Sciences and Engineering Research Council of Canada PGS-A (A.D.M.), a Heart and Stroke Richard Lewar Centre for Excellence Studentship (A.D.M.), an University of Toronto Open Studentship (A.D.M.), and an Ontario Graduate Scholarship (A.D.M.). R.M.H. holds a Canada Research Chair in Imaging; B.G.B. holds a Canada Research Chair in Developmental Cardiology.

Appendix A. Supplementary data

Supplementary data associated with this article can be found, in the online version, at doi:10.1016/j.ydbio.2006.05.023.

References

Basson, C.T., Bachinsky, D.R., Lin, R.C., Levi, T., Elkins, J.A., Soults, J., Grayzel, D., Kroumpouzou, E., Traill, T.A., Leblanc-Straceski, J., Renault, B., Kucherlapati, R., Seidman, J.G., Seidman, C.E., 1997. Mutations in human TBX5 cause limb and cardiac malformation in Holt–Oram syndrome. Nat. Genet. 15, 30–35.

Basson, C.T., Huang, T., Lin, R.C., Bachinsky, D.R., Weremowicz, S., Vaglio, A., Bruzzone, R., Quadrelli, R., Lerone, M., Romeo, G., Silengo, M., Pereira, A., Krieger, J., Mesquita, S.F., Kamisago, M., Morton, C.C., Pierpont, M.E., Muller, C.W., Seidman, J.G., Seidman, C.E., 1999. Different TBX5 interactions in heart and limb defined by Holt–Oram syndrome mutations. Proc. Natl. Acad. Sci. U. S. A. 96, 2919–2924.

Benson, D.W., Silberbach, G.M., Kavanaugh-McHugh, A., Cottrill, C., Zhang, Y., Riggs, S., Smalls, O., Johnson, M.C., Watson, M.S., Seidman, J.G., Seidman, C.E., Plowden, J., Kugler, J.D., 1999. Mutations in the cardiac transcription factor NKX2.5 affect diverse cardiac developmental pathways. J. Clin. Invest. 104, 1567–1573.

Brassington, A.M., Sung, S.S., Toydemir, R.M., Le, T., Roeder, A.D., Rutherford, A.E., Whitby, F.G., Jorde, L.B., Bamshad, M.J., 2003. Expressivity of Holt–Oram syndrome is not predicted by TBX5 genotype. Am. J. Hum. Genet. 73, 74–85.

Bruneau, B.G., 2002. Transcriptional regulation of vertebrate cardiac morphogenesis. Circ. Res. 90, 509–519.

Bruneau, B.G., Logan, M., Davis, N., Levi, T., Tabin, C.J., Seidman, J.G., Seidman, C.E., 1999. Chamber-specific cardiac expression of Tbx5 and heart defects in Holt–Oram syndrome. Dev. Biol. 211, 100–108.

Bruneau, B.G., Nemer, G., Schmitt, J.P., Charron, F., Robitaille, L., Caron, S., Conner, D.A., Gessler, M., Nemer, M., Seidman, C.E., Seidman, J.G., 2001. A murine model of Holt–Oram syndrome defines roles of the T-box transcription factor Tbx5 in cardiogenesis and disease. Cell 106, 709–721.

Christoffels, V.M., Keijser, A.G., Houweling, A.C., Clout, D.E., Moorman, A.F., 2000. Patterning the embryonic heart: identification of five mouse Iroquois homeobox genes in the developing heart. Dev. Biol. 224, 263–274.

Davidson, E.H., 2002. Genomic Regulatory Systems: Development and Evolution. Academic Press, San Diego.

Epstein, J.A., Buck, C.A., 2000. Transcriptional regulation of cardiac development: implications for congenital heart disease and DiGeorge syndrome. Pediatr. Res. 48, 717–724.

Garg, V., Kathiriya, I.S., Barnes, R., Schluterman, M.K., King, I.N., Butler, C. A., Rothrock, C.R., Eapen, R.S., Hirayama-Yamada, K., Joo, K., Matsuoka, R., Cohen, J.C., Srivastava, D., 2003. GATA4 mutations cause human congenital heart defects and reveal an interaction with TBX5. Nature 424, 443–447.

Gibson-Brown, J.J., S.I.A., Silver, L.M., Papaioannou, V.E., 1998. Expression of T-box genes Tbx2–Tbx5 during chick organogenesis. Mech. Dev. 74, 165–169.

Goering, L.M., Hoshijima, K., Hug, B., Bisgrove, B., Kispert, A., Grunwald, D.J., 2003. An interacting network of T-box genes directs gene expression and fate in the zebrafish mesoderm. Proc. Natl. Acad. Sci. U. S. A. 100, 9410–9415.

Gruber, P.J., Epstein, J.A., 2004. Development gone awry: congenital heart disease. Circ. Res. 94, 273–283.

Habets, P.E., Moorman, A.F., Clout, D.E., van Roon, M.A., Lingbeek, M., van Lohuizen, M., Campione, M., Christoffels, V.M., 2002. Cooperative action of Tbx2 and Nkx2.5 inhibits ANF expression in the atrioventricular canal: implications for cardiac chamber formation. Genes Dev. 16, 1234–1246.

Hoogaars, W.M., Tessari, A., Moorman, A.F., de Boer, P.A., Hagoort, J., Soufan, A.T., Campione, M., Christoffels, V.M., 2004. The transcriptional repressor Tbx3 delineates the developing central conduction system of the heart. Cardiovasc. Res. 62, 489–499.

Huang, T., Lock, J.E., Marshall, A.C., Basson, C., Seidman, J.G., Seidman, C.E., 2002. Causes of clinical diversity in human TBX5 mutations. Cold Spring Harbor Symp. Quant. Biol. 67, 115–120.

Irizarry, R.A., Hobbs, B., Collin, F., Beazer-Barclay, Y.D., Antonellis, K.J., Scherf, U., Speed, T.P., 2003. Exploration, normalization, and summaries of high density oligonucleotide array probe level data. Biostatistics 4, 249–264.

Jerome, L.A., Papaioannou, V.E., 2001. DiGeorge syndrome phenotype in mice mutant for the T-box gene, Tbx1. Nat. Genet. 27, 286–291.

Koshiba-Takeuchi, K., Takeuchi, J.K., Arruda, E.P., Kathiriya, I.S., Mo, R., Hui, C.C., Srivastava, D., Bruneau, B.G., 2006. Cooperative and antagonistic interactions between Sall4 and Tbx5 pattern the mouse limb and heart. Nat. Genet. 38, 175–183.

Li, Q.Y., Newbury-Ecob, R.A., Terrett, J.A., Wilson, D.I., Curtis, A.R., Yi, C.H., Gebuhr, T., Bullen, P.J., Robson, S.C., Strachan, T., Bonnet, D., Lyonnet, S., Young, I.D., Raeburn, J.A., Buckler, A.J., Law, D.J., Brook, J.D., 1997. Holt–Oram syndrome is caused by mutations in TBX5, a member of the Brachyury (T) gene family. Nat. Genet. 15, 21–29.

Lickert, H., Kutsch, S., Kanzler, B., Tamai, Y., Taketo, M.M., Kemler, R., 2002. Formation of multiple hearts in mice following deletion of beta-catenin in the embryonic endoderm. Dev. Cell 3, 171–181.

Lickert, H., Takeuchi, J.K., Von Both, I., Walls, J.R., McAuliffe, F., Adamson, S.L., Henkelman, R.M., Wrana, J.L., Rossant, J., Bruneau, B.G., 2004. Baf60c is essential for function of BAF chromatin remodelling complexes in heart development. Nature 432, 107–112.

Lindsay, E.A., Vitelli, F., Su, H., Morishima, M., Huynh, T., Pramparo, T., Jurecic, V., Ogunrinu, G., Sutherland, H.F., Scambler, P.J., Bradley, A., Baldini, A., 2001. Tbx1 haploinsufficiency in the DiGeorge syndrome region causes aortic arch defects in mice. Nature 410, 97–101.

Livak, K.J., Schmittgen, T.D., 2001. Analysis of relative gene expression data using real-time quantitative PCR and the 2(-Delta Delta C(T)) method. Methods 25, 402–408.

Markstein, M., Zinzen, R., Markstein, P., Yee, K.P., Erives, A., Stathopoulos, A., Levine, M., 2004. A regulatory code for neurogenic gene expression in the *Drosophila* embryo. Development 131, 2387–2394.

Marvin, M.J., Di Rocco, G., Gardiner, A., Bush, S.M., Lassar, A.B., 2001. Inhibition of Wnt activity induces heart formation from posterior mesoderm. Genes Dev. 15, 316–327.

Merscher, S., Funke, B., Epstein, J.A., Heyer, J., Puech, A., Lu, M.M., Xavier, R.J., Demay, M.B., Russell, R.G., Factor, S., Tokooya, K., Jore, B.S., Lopez, M., Pandita, R.K., Lia, M., Carrion, D., Xu, H., Schorle, H., Kobler, J.B., Scambler, P., Wynshaw-Boris, A., Skoultchi, A.I., Morrow, B.E., Kucherlapati, R., 2001. TBX1 is responsible for cardiovascular defects in velo-cardio-facial/DiGeorge syndrome. Cell 104, 619–629.

Meyers, E.N., Lewandoski, M., Martin, G.R., 1998. An Fgf8 mutant allelic series generated by Cre- and Flp-mediated recombination. Nat. Genet. 18, 136–141.

Moorman, A.F., Soufan, A.T., Hagoort, J., de Boer, P.A., Christoffels, V.M., 2004. Development of the building plan of the heart. Ann. N. Y. Acad. Sci. 1015, 171–181.

Mori, A.D., Bruneau, B.G., 2004. TBX5 mutations and congenital heart disease: Holt–Oram syndrome revealed. Curr. Opin. Cardiol. 19, 211–215.

Murakami, M., Nakagawa, M., Olson, E.N., Nakagawa, O., 2005. A WW domain protein TAZ is a critical coactivator for TBX5, a transcription factor implicated in Holt–Oram syndrome. Proc. Natl. Acad. Sci. U. S. A. 102, 18034–18039.

Okubo, A., Miyoshi, O., Baba, K., Takagi, M., Tsukamoto, K., Kinoshita, A., Yoshiura, K., Kishino, T., Ohta, T., Niikawa, N., Matsumoto, N., 2004. A novel GATA4 mutation completely segregated with atrial septal defect in a large Japanese family. J. Med. Genet. 41, E97.

Ovcharenko, I., Loots, G.G., Giardine, B.M., Hou, M., Ma, J., Hardison, R.C., Stubbs, L., Miller, W., 2005. Mulan: multiple-sequence local alignment and visualization for studying function and evolution. Genome Res. 15, 184–194.

Pocock, R., Ahringer, J., Mitsch, M., Maxwell, S., Woollard, A., 2004. A regulatory network of T-box genes and the even-skipped homologue vab-7 controls patterning and morphogenesis in *C. elegans*. Development 131, 2373–2385.

Qian, L., Liu, J., Bodmer, R., 2005. Slit and robo control cardiac cell polarity and morphogenesis. Curr. Biol. 15, 2271–2278.

Rossi, F.M., Kringstein, A.M., Spicher, A., Guicherit, O.M., Blau, H.M., 2000. Transcriptional control: rheostat converted to on/off switch. Mol. Cell 6, 723–728.

Schott, J.J., Benson, D.W., Basson, C.T., Pease, W., Silberbach, G.M., Moak, J.P., Maron, B.J., Seidman, C.E., Seidman, J.G., 1998. Congenital heart disease caused by mutations in the transcription factor NKX2-5. Science 281, 108–111.

Seidman, J.G., Seidman, C., 2002. Transcription factor haploinsufficiency: when half a loaf is not enough. J. Clin. Invest. 109, 451–455.

Sharpe, J., Ahlgren, U., Perry, P., Hill, B., Ross, A., Hecksher-Sorensen, J., Baldock, R., Davidson, D., 2002. Optical projection tomography as a tool for 3D microscopy and gene expression studies. Science 296, 541–545.

Srivastava, D., Olson, E.N., 2000. A genetic blueprint for cardiac development. Nature 407, 221–226.

Sun, G., Lewis, L.E., Huang, X., Nguyen, Q., Price, C., Huang, T., 2004. TBX5, a gene mutated in Holt–Oram syndrome, is regulated through a GC box and T-box binding elements (TBEs). J. Cell. Biochem. 92, 189–199.

Takeuchi, J.K., Mileikovskaia, M., Koshiba-Takeuchi, K., Heidt, A.B., Mori, A.D., Arruda, E.P., Gertsenstein, M., Georges, R., Davidson, L., Mo, R., Hui, C.C., Henkelman, R.M., Nemer, M., Black, B.L., Nagy, A., Bruneau, B.G., 2005. Tbx20 dose-dependently regulates transcription factor networks required for mouse heart and motoneuron development. Development 132, 2463–2474.

Tzahor, E., Lassar, A.B., 2001. Wnt signals from the neural tube block ectopic cardiogenesis. Genes Dev. 15, 255–260.

Wu, J.Y., Feng, L., Park, H.T., Havlioglu, N., Wen, L., Tang, H., Bacon, K.B., Jiang, Z., Zhang, X., Rao, Y., 2001. The neuronal repellent Slit inhibits leukocyte chemotaxis induced by chemotactic factors. Nature 410, 948–952.

Wu, Z., Irizarry, R.A., 2004. Preprocessing of oligonucleotide array data. Nat. Biotechnol. 22, 656–658 (author reply 658).

Xu, L., Corcoran, R.B., Welsh, J.W., Pennica, D., Levine, A.J., 2000. WISP-1 is a Wnt-1- and beta-catenin-responsive oncogene. Genes Dev. 14, 585–595.

Xu, X., Li, C., Garrett-Beal, L., Larson, D., Wynshaw-Boris, A., Deng, C.X., 2001. Direct removal in the mouse of a floxed neo gene from a three-loxP conditional knockout allele by two novel approaches. Genesis 30, 1–6.

Yagi, H., Furutani, Y., Hamada, H., Sasaki, T., Asakawa, S., Minoshima, S., Ichida, F., Joo, K., Kimura, M., Imamura, S., Kamatani, N., Momma, K., Takao, A., Nakazawa, M., Shimizu, N., Matsuoka, R., 2003. Role of TBX1 in human del22q11.2 syndrome. Lancet 362, 1366–1373.

Yamada, M., Revelli, J.P., Eichele, G., Barron, M., Schwartz, R.J., 2000. Expression of chick Tbx-2, Tbx-3, and Tbx-5 genes during early heart development: evidence for BMP2 induction of Tbx2. Dev. Biol. 228, 95–105.

Zhou, Y.Q., Davidson, L., Henkelman, R.M., Nieman, B.J., Foster, F.S., Yu, L.X., Chen, X.J., 2004. Ultrasound-guided left-ventricular catheterization: a novel method of whole mouse perfusion for microimaging. Lab. Invest. 84, 385–389.